PNL-5904-1
UC-70

2F

LFCM Vitrification Technology

Quarterly Progress Report
October-December 1985

H. C. Burkholder, J. H. Jarrett,
and J. E. Minor, Compilers

September 1986

Prepared for the U.S. Department of Energy
under Contract DE-AC06-76RLO 1830

Pacific Northwest Laboratory
Operated for the U.S. Department of Energy
by Battelle Memorial Institute

Battelle

PNL-5904-1

DISCLAIMER

PACIFIC NORTHWEST LABORATORY
operated by
BATTELLE
for the
UNITED STATES DEPARTMENT OF ENERGY
under Contract DE-AC06-76RLO 1830

Printed in the United States of America
Available from
National Technical Information Service
United States Department of Commerce
5285 Port Royal Road
Springfield, Virginia 22151

NTIS Price Codes
Microfiche A01

Printed Copy

Pages	Price Codes
001-025	A02
026-050	A03
051-075	A04
076-100	A05
101-125	A06
126-150	A07
151-175	A08
176-200	A09
201-225	A010
226-250	A011
251-275	A012
276-300	A013

PNL-5904-1
UC-70

LFCM VITRIFICATION TECHNOLOGY

QUARTERLY PROGRESS REPORT

October-December 1985

H. C. Burkholder, J. H. Jarrett,
and J. E. Minor,.Compilers

Contributing Authors

C. M. Anderson
S. O. Bates
H. T. Blair
L. R. Bunnell
R. D. Dierks
L. J. Ethridge
D. W. Faletti
R. K. Farnsworth
R. W. Goles
W. L. Kuhn
G. D. Maupin
R. K. Nakaoka
W. L. Partain
J. M. Perez, Jr.
M. E. Peterson
P. W. Reimus
K. J. Schneider
G. J. Sevigny
J. W. Shade
D. H. Siemens

September 1986

Prepared for
the U.S. Department of Energy
under Contract DE-AC06-76RLO 1830

Pacific Northwest Laboratory
Richland, Washington 99352

ABSTRACT

This report is compiled by the Nuclear Waste Treatment Program and the Hanford Waste Vitrification Program at Pacific Northwest Laboratory to document progress on liquid-fed ceramic melter (LFCM) vitrification technology. Progress in the following technical subject areas during the first quarter of FY 1986 is discussed: melting process chemistry and glass development, feed preparation and transfer systems, melter systems, canister filling and handling systems, off-gas systems, process/product modeling and control, and supporting studies.

SUMMARY

This report is compiled by the Nuclear Waste Treatment Program (NWTP) and the Hanford Waste Vitrification Program (HWVP) to describe the progress in developing, testing, applying, and documenting liquid-fed ceramic melter (LFCM) vitrification technology. Activities in the first quarter of FY 1986 are summarized below:

Melting Process Chemistry and Glass Development - Thirty melter feed test batches were evaluated for sediment formation after standing undisturbed for approximately 1-1/2 months. Although none of the batches developed a sediment layer, all batches exhibited some degree of gelling, which could be correlated with the amount of formic acid used in feed treatment during the batch processing. The effects of boiling on the rheological properties of simulated HWVP melter feeds were evaluated. Whether or not a melter feed was boiled had little effect on the yield stress and apparent viscosity at concentrations below 550 g total oxides/liter (TO/L) but boiling had an effect at concentrations of 600 g TO/L. The waste variability study results predicted that with a 25 wt% total waste loading (ZrO_2 + waste) the glass could contain up to 10 wt% ZrO_2 (40 wt% in the waste) before the temperature at which the viscosity reaches 100 poise exceeds 1150°C. The addition of ZrO_2 to the glass over the range tested increased the durability of the glass.

Feed Preparation and Transfer Systems - A detailed test procedure was prepared to characterize and evaluate the resuspension of melter feed slurries in pipes. The testing will involve characterizing the physical properties of the solid and liquid phases of the slurry, the piping system using Newtonian fluids, the piping system using fully suspended slurry, and the slurry flow over a sediment bed.

Melter Systems - Off-gas data analysis from the operation of the nonradioactive pilot-scale ceramic melter (PSCM) showed that most melter off-gas losses were associated with aerosol emission. Equipment performance data and decontamination factors were determined for the major components as well as Cs, S, and Ru.

Canister Filling and Handling Systems - The limited technical progress that took place this quarter will be reported in a future quarterly report.

Off-Gas Systems - Melter emission and off-gas system performance studies have been conducted to evaluate the LFCM processing system. The overall system decontamination factors established during testing were lower than expected primarily because of high formate-induced cesium volatility and inadequate performance of the high-efficiency scrubbers that were used.

Process/Product Modeling and Control - A commercially available simulation language has been adapted for use in modeling a simple vitrification process. Plans for improving and upgrading the ability of the TEMPEST heat transfer code to analyze the filling and cooling of canisters are discussed. Correlations for predicting the extent of cracking in glass castings produced by LFCMs have been developed.

Supporting Studies - The overview report of the West Valley vitrification system design provides the design bases and rationale for the equipment design. This perspective is useful for the West Valley Project and for transfer of technology to other applications. One high-temperature glass, EMS-11, appears to have the potential of being a viable, significantly superior second-generation waste form. Data collection continues for use in modeling chemical durability behavior. Synroc-C appears to be a better waste form than a PNL 76-68 type of borosilicate glass based on leach test performance but not necessarily on waste loading capacity.

CONTENTS

FIGURES

TABLES

INTRODUCTION

In mid-FY 1982, the U.S. Department of Energy (DOE) assigned responsibility for managing its commercial nuclear waste treatment activities in the United States to the Nuclear Waste Treatment Program (NWTP) at Pacific Northwest Laboratory (PNL).[a] The NWTP establishes the technology for treating and immobilizing high-level waste (HLW), transuranic waste (TRUW), and other related wastes. This work includes developing waste treatment system technology and components, testing treatment systems, verifying the operability of the technologies through practical applications, producing waste packages for storage and disposal testing, assisting others to resolve specific problems in transferring the developed technologies, and maintaining a resource of radioactive waste treatment capabilities and facilities for DOE.

Major current activities include: developing waste glass formulations and vitrification equipment for HLW; operating a pilot-scale liquid-fed ceramic melter (LFCM) system under radioactive conditions; designing, fabricating, and installing canister closure, decontamination, destructive and nondestructive examination, and storage facilities for vitrified radioactive waste; providing heat and radiation sources to the Federal Republic of Germany (FRG) Asse Mine Test; developing and testing TRUW and second-generation HLW treatment technology; and providing processing technology and vitrification process equipment for treating West Valley wastes. These activities support the longer term goals of completing system design and operations documentation and production specifications for HLW treatment (vitrification) by 1992, for TRUW treatment by 1996, and for second-generation HLW treatment by 2000.

The NWTP is multifunded with base program funds from DOE-Nuclear Energy (NE) and user funding supplied by DOE-NE-West Valley (DOE-NE-WV), DOE-Defense Programs-Richland (DOE-DP-RL), FRG, and Japan. The NWTP is managed by H. C. Burkholder and J. H. Jarrett. The program is divided into the following tasks:

(a) Operated for DOE by Battelle Memorial Institute under Contract DE-AC06-76RLO 1830.

- Technology Development - W. A. Ross
- Technology Testing - R. A. Brouns
- RLFCM Operations - W. J. Bjorklund
- A-Cell Facility Preparation - G. H. Bryan
- West Valley Support - J. R. Carrell.

Progress in all program elements is reported through informal monthly status reports, formal annual reports (McElroy and Burkholder 1984; Burkholder and Rusin 1985; Burkholder and Jarrett 1986), and formal topical reports. Recognizing both the magnitude of the first-generation HLW program element and the large number of applications currently under way, this quarterly report series was begun in FY 1985 to facilitate the transfer of LFCM vitrification technology between and among the central source (PNL) and the various user groups: the Waste Valley Demonstration Project (WVDP), the Hanford Waste Vitrification Program (HWVP), and the Defense Waste Processing Facility (DWPF) Project. Quarterly reports will be established for other program elements as the need arises.

The results of applicable technical work performed by PNL in direct support of the HWVP are included in this report. The HWVP is being conducted by Rockwell Hanford Operations (RHO) for DOE; DOE and RHO have assigned to PNL the responsibility for development of vitrification system technology for application to the HWVP. The HWVP facility, one of three major U.S. vitrification facilities for defense HLW and TRUW, will use PNL-developed vitrification technology. This technology will also be used for the DWPF and the WVDP. Progress in the development of waste- and site-specific technologies is presented in this quarterly report to complement NWTP-supported activities. The PNL HWVP work is managed by J. E. Minor.

Because the emphasis of these quarterly reports is technical rather than programmatic, the reports are organized to cover technical subject areas without regard to funding sources. This quarterly is organized as follows:

- Melting Process Chemistry and Glass Development - S. O. Bates
- Feed Preparation and Transfer Systems - M. E. Peterson
- Melter Systems - R. D. Dierks and J. M. Perez, Jr.
- Canister Filling and Handling Systems - D. H. Siemens

- Off-Gas Systems - R. W. Goles
- Process/Product Modeling and Control - W. L. Kuhn
- Supporting Studies - K. J. Schneider.

Each section contains summary, introduction, and technical progress subsections. The reports are compiled by H. C. Burkholder, J. H. Jarrett, and J. E. Minor and edited by S. K. Edler.

REFERENCES

Burkholder, H. C., and J. H. Jarrett, Compilers. 1986. Nuclear Waste Treatment Program, Annual Report for FY 1985. PNL-5787, Pacific Northwest Laboratory, Richland, Washington.

Burkholder, H. C., and J. M. Rusin, Compilers. 1985. Nuclear Waste Treatment Program, Annual Report for FY 1984. PNL-5414, Pacific Northwest Laboratory, Richland, Washington.

McElroy, J. L., and H. C. Burkholder, Compilers. 1984. Commercial Waste Treatment Program, Annual Report for FY 1983. PNL-4963, Pacific Northwest Laboratory, Richland, Washington.

MELTING PROCESS CHEMISTRY AND GLASS DEVELOPMENT

S. O. Bates and H. T. Blair

SUMMARY

Work conducted this quarter centered on the Hanford Waste Vitrification Program (HWVP). The frit that is added to HWVP feed to produce a glass was characterized to determine those physical properties required for flowsheet calculations and for the design work to be performed by the architect-engineers.

Thirty melter feed test batches prepared for the melter feed concentration study described in the last quarterly report (Burkholder, Jarrett, and Minor 1986) were evaluated for sediment formation after standing undisturbed for approximately 1-1/2 months. None of the batches developed a sediment layer, but they had all gelled to various degrees. The extent of gelling could be correlated with the amount of formic acid used to treat the simulated HWVP feed during the batch processing. Gelling decreased as the amount of acid increased.

A scoping study was completed to evaluate the effects of boiling versus not boiling on the rheological properties of simulated HWVP melter feeds as part of the preparation process. Whether or not a melter feed was boiled had little effect on the yield stress and apparent viscosity at concentrations below 550 g TO/L (total oxides/liter), but it had an effect at concentrations of 600 g TO/L. Boiling had a significant effect on the pH of the melter feed, but rheological properties do not appear to be a function of pH in the pH range studied except at a concentration of 600 g TO/L.

A waste variability study using the HWVP reference glass composition (HW39) was completed to evaluate the changes in critical glass and melt properties due to changes in the ZrO_2 content and waste loading of a Hanford defense liquid high-level and transuranic waste (neutralized current acid waste or NCAW). The results predict that with a 25 wt% total waste loading (ZrO_2 + other waste) the glass could contain up to 10 wt% ZrO_2 (40 wt% in the waste)

before the temperature at which the viscosity of the glass reaches 100 poise (T100P) exceeds 1150°C, which is the upper limit for melter operation. Within the more restrictive composition range required to produce an acceptable T100P, the electrical conductivity of the glass melt at 1150°C (E1150) is well within the required limits. The addition of ZrO_2 to the glass over the range tested increased the durability of the glass.

INTRODUCTION

The objectives of this work are to develop glass compositions that will produce glass products having acceptable chemical durability and to design feed formulations that can be processed in a liquid-fed ceramic melter (LFCM) at an acceptable rate. Glass-forming chemicals and other chemicals used for redox control are selected to maximize melting performance and minimize problems due to foaming, metal precipitation, and other adverse phase separation. The resulting glass composition is designed to have a viscosity of 100 poise and an electrical conductivity between 0.18 and 0.5 $(ohm\text{-}cm)^{-1}$ in the temperature region between 1070°C and 1150°C. In addition, the glass is designed to minimize the tendency to form crystals above 900°C or other secondary phases on the melt surface.

The key product property is chemical durability. Specifications for chemical durability of waste glass as determined by laboratory tests have not been defined. Existing regulations pertain to radionuclide release from the controlled zone of the repository. Thus, a prudent development strategy is to assume that the chemical durability, as measured by laboratory tests, should be as high as possible within the other processing constraints.

The technical approach involves a close interaction among feed formulation, glass composition, and waste processing work being conducted at Pacific Northwest Laboratory (PNL). Hence, a glass composition is being developed to provide the appropriate high-temperature properties (viscosity, electrical conductivity) and low-temperature properties (elemental release rate, crystallization rate). Nitrate, oxide, and hydroxide chemicals representing the waste fraction and glass-forming chemicals are made into a slurry in the laboratory.

The redox state of the glass is then optimized using a reducing agent in the slurry until the ferrous/ferric ratio in the melted glass is between 0.005 and 0.3. Then, the melting rate of this feed is determined using the bottom-heated crucible test in the laboratory, which measures the rate at which the cold cap formed from this feed melts on molten glass.

Several variations are examined and the feed formulation with the best melting characteristics in this rapid, inexpensive test is recommended for short-term testing in an experimental-scale melter. If problems occur, additional laboratory glass composition or feed formulation work is conducted. A successful short-term test leads to the development of an extended test in the pilot-scale ceramic melter (PSCM) or high-bay ceramic melter (HBCM).

Applicable technology developed in the HWVP is also presented in this section. The HWVP is dedicated to the vitrification of the liquid high-level and transuranic defense wastes produced and stored at the Hanford Site, near Richland, Washington. The objectives of the HWVP are to:

- Develop reference glass formulations incorporating the different waste streams to be processed through HWVP. These glass compositions should have the required physical properties for processing in an LFCM (viscosity, electrical conductivity, and phase behavior) and the maximum chemical durability.
- Evaluate the effects of possible variations of selected waste components on the physical properties and chemical durability of the reference glass.
- Prepare a simulation of the HWVP reference feeds that represents the true chemical and physical properties of the waste, with the exception of radiation and heat generation, and creates no artificial difficulties.
- Determine ways to modify the rheology of the melter feed to improve homogeneity and minimize transport difficulties.

- Conduct laboratory-scale feed rheological property adjustment studies in support of feed process and composition variability testing, melter feed optimization, and evaluation of feed processing analytical requirements.
- Document laboratory- and engineering-scale testing of the effects of process and waste composition variability on feed rheological and redox properties.

TECHNICAL PROGRESS

During this quarter, efforts involved the evaluation of the rheological properties of the HWVP NCAW melter feed and the effects of feed processing parameters on the rheology of that feed. Work was also conducted to evaluate the effects on glass and melt properties due to ZrO_2 variability in NCAW.

MELTER FEED PROCESSING

The physical properties were measured for the glass frit that is added to simulated HWVP reference feed to produce a melter feed that yields a glass having the HW39 composition. The frit sample that was characterized was obtained from the stock used to prepare melter feed for pilot-scale ceramic melter run PSCM-22. The properties of the frit are presented in Table 1. These data are required to complete flowsheet calculations and to provide a design data base for the architect-engineers.

Thirty melter feed test batches prepared for the melter feed concentration study described in the last quarterly report (Burkholder, Jarrett, and Minor 1986) were evaluated for sediment formation after standing undisturbed for approximately 1-1/2 months. Batches 26 through 55 were contained in sealed graduated cylinders. A stirring rod was used to probe for a sediment layer. None of the 30 batches had a sediment layer.

All of the batches were found to have gelled to different degrees. They were grouped into three general categories as shown in Table 2. Some general trends can be discerned from these results. The least-gelled batches were made

TABLE 1. Frit HW39 Physical Properties[a]

Lot No.: M7673 (Used for PSCM-22)

Specified Size: -80/+200 mesh

Bulk Properties Measured:

Aerated bulk density:	1.14 g/cm^3
Packed bulk density:	1.37 g/cm^3
Average bulk density:	1.26 g/cm^3
Angle of repose:	38°
Specific density:	2.49 to 2.51 g/cm^3

Particle size distribution:

Sieve Size U.S. Std. Mesh	Cumulative wt% Under Size
80	97
100	73
120	50
140	23
170	9
200	1
Mean particle size:	120 mesh

(a) Supplier: American Porcelain Enamel Company, 1285 East Keating Avenue, Muskegon, Michigan.

TABLE 2. Degrees of Gelation of Simulated HWVP Melter Feed Test Batches

Little Gelling	Medium Gelling		Well Gelled
26	28	46	37
27	29	47	40
31	30	48	42
34	32	49	45
35	33	51	50
39	36	52	55
44	38	53	
	41	54	
	43		

with two and three times the stoichiometric amounts of formic acid while many of the well-gelled batches were made with the stoichiometric amount of formic acid.

A scoping study was completed to evaluate the effects of boiling versus not boiling on the rheological properties of simulated HWVP melter feeds. This study was performed because batches of melter feed prepared at and below concentrations of 500 g TO/L for the melter feed concentration study described in the last quarterly report were not boiled while the more concentrated batches were boiled. Eight batches were prepared as shown in Table 3.

The test batches were prepared from the same simulated HWVP reference feed batch (Batch HWS5) used to perform the melter feed concentration study. A large subbatch was treated with a stoichiometric amount of formic acid (0.092 g HCOOH/g waste oxides) using the standard procedure and then boiled to a concentration of 187 g WO/L (waste oxides/liter). A small subbatch that was not treated with HCOOH was also prepared at a concentration of 139.5 g WO/L to serve as a control.

During the concentration of the large subbatch, the effluents were passed through a water-cooled condenser that was about 60% effective. The condensate was analyzed for formic acid content and contained less than 10 ppm. This does not mean formic acid is not being driven off during the concentration operation. It only shows that formic acid was not collected with the 60% of the condensible effluents collected by the condenser. A more efficient condenser is being obtained.

TABLE 3. Matrix of Laboratory Batches of Melter Feeds Prepared to Evaluate Effects of Boiling

Concentration, g TO/L[a]	Not Boiled		Boiled 6 h	
	With HCOOH	Without HCOOH	With HCOOH	Without HCOOH
400	HWS5-1		HWS5-2	
500	HWS5-3	HWS5-7	HWS5-4	HWS5-8
600	HWS5-5		HWS5-6	

(a) TO/L = total oxide including frit and waste per liter.

The large subbatch of simulated waste concentrate was then divided into three sub-subbatches. Dry frit and an amount of formic acid equal to 1 wt% of the frit were added to each of these batches. One sub-subbatch was then diluted to a concentration of 400 g TO/L, and another was diluted to a concentration of 500 g TO/L. The third was left at a concentration of approximately 600 g TO/L. These sub-subbatches were then divided again to create simulated melter feed batches HWS5-1 through HWS5-6 as shown in Table 3. Dry frit and 1 wt% formic acid were also added to the control subbatch and it was divided to create simulated melter feed batches HWS5-7 and HWS5-8. Melter feed batches HWS5-2, -4, -6, and -8 were boiled with full reflux for 6 hours. This length of time was selected because it was the maximum boiling time required to concentrate the batches used in the concentration study.

The rheological and chemical properties of each melter feed batch were measured within 24 hours of the final step in the batch preparation. The results are presented in Table 4.

The most interesting result of this scoping study is that all batches at a concentration of 500 g TO/L and greater had dilatant fluid behavior. The shear stress in the fluid was not constant but increased as the shear rate increased, as shown in Figure 1. This type of fluid behavior is the most undesirable for a melter feed because the fluid will become more resistant to flow as the motivating force is increased to increase flow. Plugs that form in transfer and feed lines will become more resistant to flow as pressure is increased in an effort to flush the lines. Figure 1 also shows that the dilatant behavior is shear dependent and that the fluid becomes pseudoplastic after being agitated. Further studies are being performed to see if the dilatant behavior can be eliminated by adding formic acid or by exposing the fluid to higher shear rates.

The data presented in Table 4 were plotted in several different ways along with selected data from the concentration study to determine what effect boiling simulated melter feed has on the rheological properties (Figures 2 through 5). The data from the concentration study are from the batches made with stoichiometric amounts of formic acid and the -80/+200 mesh frit unless

TABLE 4. Properties of Simulated Melter Feed Batches Prepared to Evaluate the Effects of Boiling

Properties	HWS5-1	HWS5-2	HWS5-3	HWS5-4	HWS5-5	HWS5-6	HWS5-7	HWS5-8
Boil time, h	0	6	0	6	0	6	0	6
Initial pH	4.40	4.40	4.33	4.33	4.42	4.42	8.78	8.78
pH after 24 h	4.98	8.45	5.28	8.32	5.50	8.34	9.28	10.50
Density, g/mL	1.27	1.27	1.33	1.33	1.41	1.42	1.32	1.33
Total solids at 105°C, wt%	34.65	34.13	40.44	40.22	47.28	47.89	40.95	41.00
Total oxides, wt%	31.97	31.22	37.20	36.96	43.65	44.00	37.88	37.79
Total oxides, g TO/L	406.1	396.6	497.8	491.6	615.5	624.8	500.1	502.7
Viscosity at 183 s^{-1}, cP	11.5	6.3	33.3	35.1	170.8	87.1	33.3	47.5
Yield point, $dynes/cm^2$	10	9	39	44	122	164	26	101
Dissolved solids, wt%	2.69	3.17	3.60	3.55	3.69	4.50	2.98	4.92
Suspended solids, wt%	32.16	30.76	32.79	36.43	43.40	43.05	37.87	37.48
Type of fluid	Pseudo-plastic	Bingham	Mild dilatant	Very dilatant	Very dilatant	Very dilatant	Mild dilatant	Mild dilatant
Fe^{+2}/Fe^{+3}	<0.005	<0.005	<0.005	<0.005	<0.005	<0.005	<0.005	<0.005

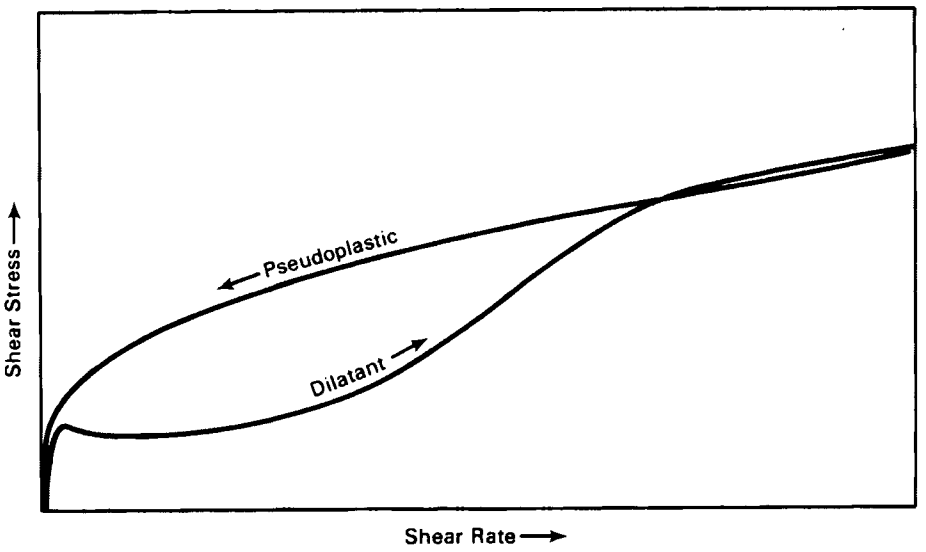

FIGURE 1. Rheogram for Simulated Melter Feed Batch HWS5-4 Showing Dilatant Fluid Behavior

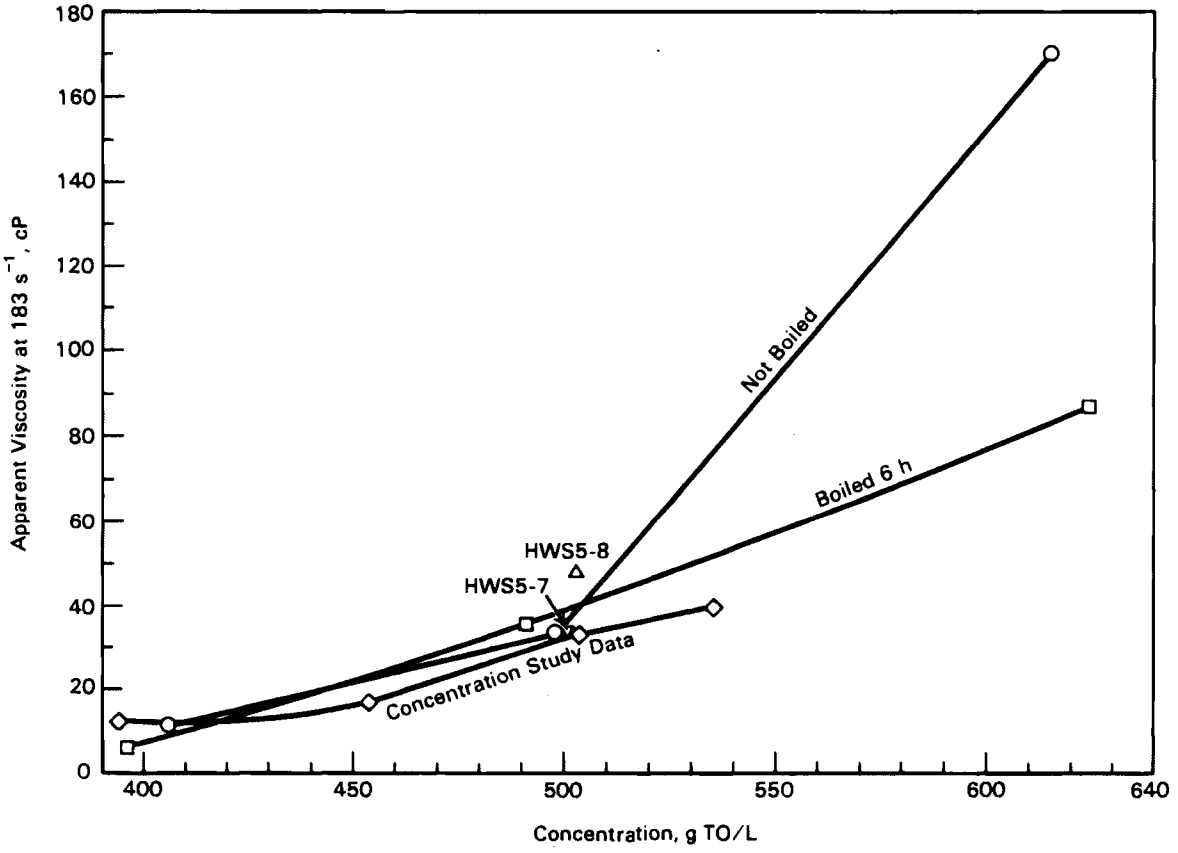

FIGURE 2. Apparent Viscosity as a Function of Concentration for Boiled and Not Boiled Melter Feeds

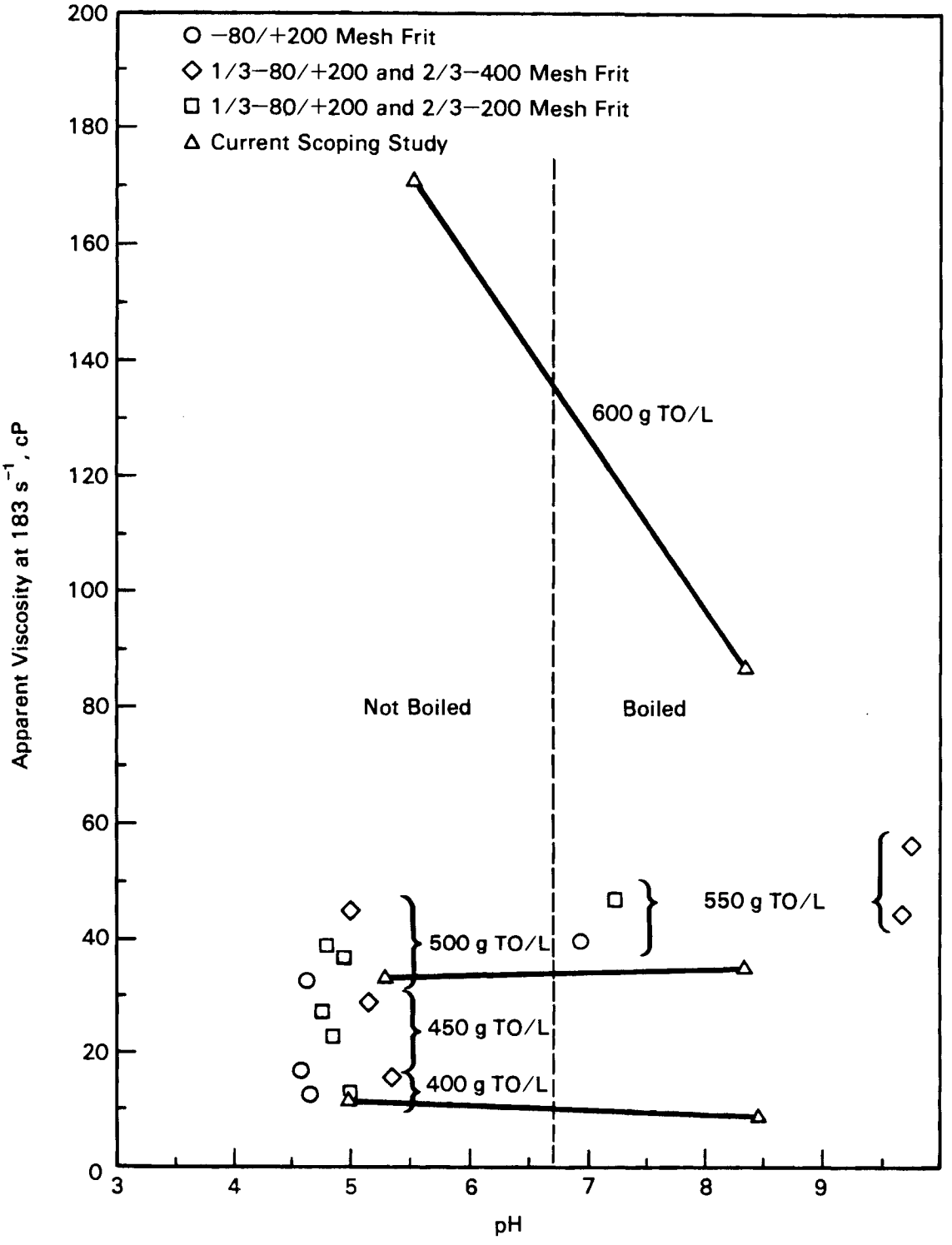

FIGURE 3. Apparent Viscosity of Melter Feeds as a Function of pH, Concentration, and Boiling Versus Not Boiling

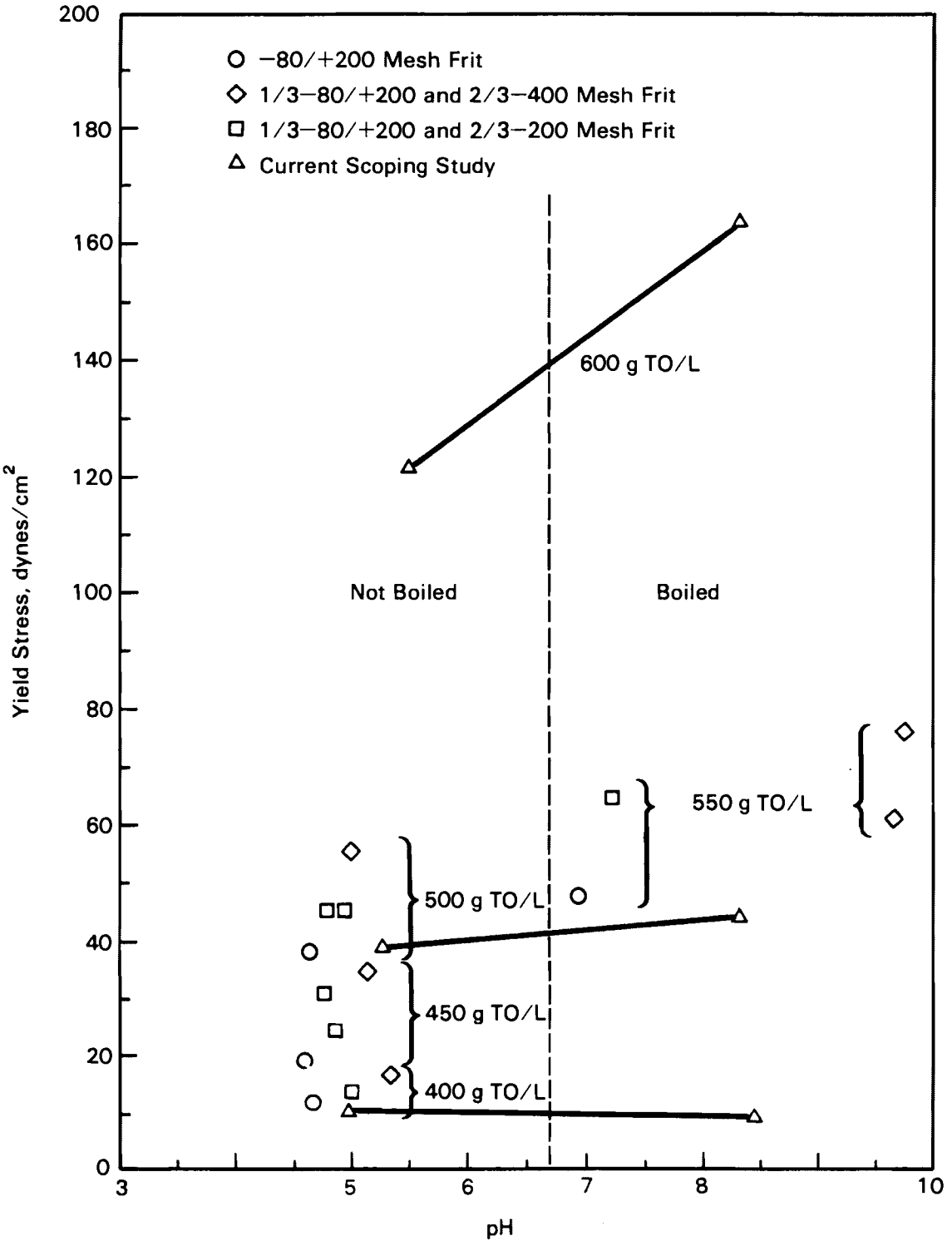

FIGURE 4. Yield Stress of Melter Feeds as a Function of pH, Concentration, and Boiling Versus Not Boiling

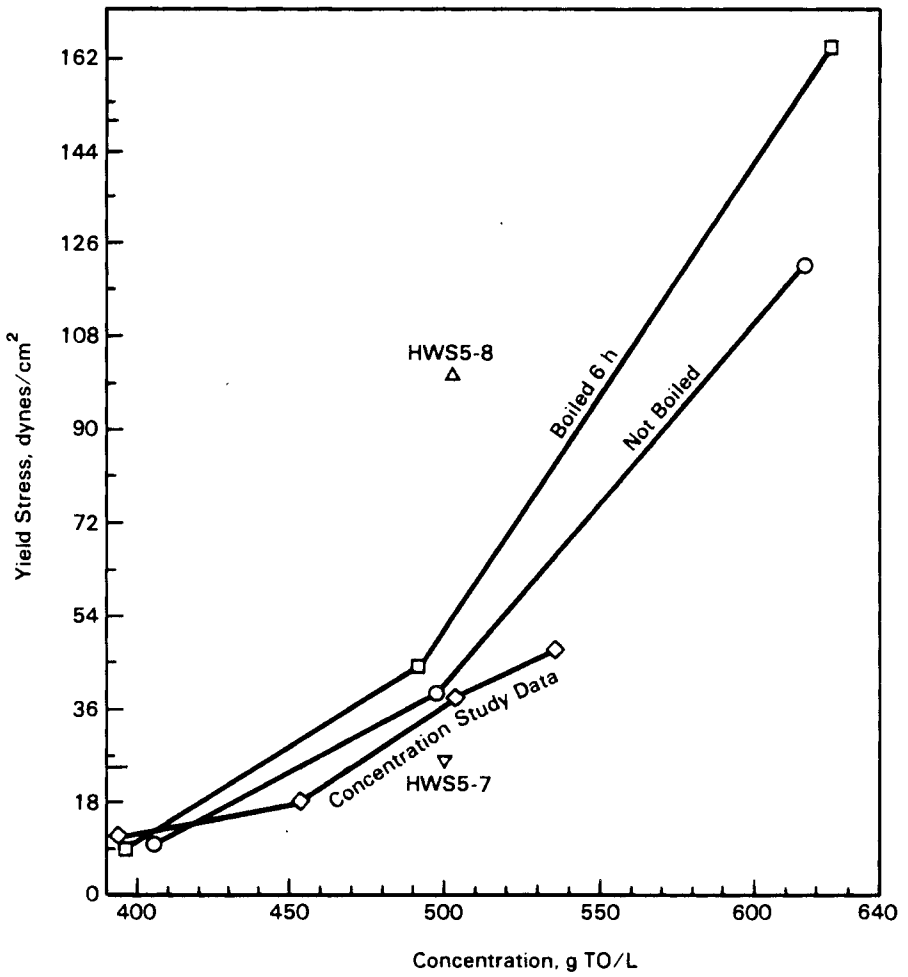

FIGURE 5. Yield Stress as a Function of Concentration for Boiled and Not Boiled Melter Feeds

otherwise indicated. It appears that boiling a melter feed has little effect on the yield stress and apparent viscosity at concentrations below 550 g TO/L but has an effect at concentrations of 600 g TO/L. The rheograms (plots of shear stress versus shear rate) for each batch suggest that boiling increases the dilatant behavior. Boiling does have a significant effect on the pH of the melter feed, but rheological properties do not appear to be a function of pH in the pH range studied except at concentrations of 600 g TO/L. These results suggest that the data obtained during the melter feed concentration study are valid for the batches that were not boiled, i.e., batches made at concentrations of 400 to 500 g TO/L.

ZrO_2 VARIABILITY

The chemical composition of NCAW to be processed through the Hanford Waste Vitrification Plant (HWVP) is expected to vary due to process changes and/or upsets. The resulting glass product will therefore deviate from the nominal composition of the reference glass. While borosilicate glasses are generally forgiving, changes in the glass composition due to variation in the feed composition can adversely affect the physical properties and/or the chemical durability of the glass. The goal of HWVP composition variability testing is to characterize the effects that given variations of selected waste components have on key glass properties. The range of composition variance allowable with acceptable alteration of the physical and chemical properties of the glass can then be predicted.

Experimental Objective and Design

The objective of the ZrO_2 variability study was to investigate and characterize the effects on critical glass and melt properties due to varying the proportions (wt%) of ZrO_2, waste without ZrO_2, and a blend of glass formers over the ranges shown in Table 5. These ranges are based on the maximum variability anticipated in NCAW. In the HWVP, the glass formers will be in the form of a glass frit, and the total waste loading is assumed to be the sum of both the ZrO_2 and the waste-ZrO_2. The total waste loading in the HWVP reference glass (HW39) is 25 wt%.

The following critical glass and melt properties were evaluated: viscosity expressed as the 100 poise temperature (T100P), electrical conductivity at 1150°C (E1150), and the chemical durability of the glasses evaluated using MCC-1 and MCC-3 leach tests.

TABLE 5. Experimental Ranges of the Three Components

Component	Minimum wt%	Maximum wt%
Glass Formers	70	85
ZrO_2	0	15
Waste-ZrO_2	0	30

The experimental design strategy was to determine an optimal set of mixtures of the three components to include in the experiment to obtain data for fitting a special cubic Scheffe polynomial model for each property. With the three components in this study, the special cubic polynomial model has the form:

$$Y = B_1(G) + B_2(Z) + B_3(W) + B_{12}(G)(Z) + B_{13}(G)(W) + B_{23}(Z)(W) + B_{123}(G)(Z)(W) + e \quad (1)$$

where Y = property

G, Z, W = pseudo-components (defined below)

e = residual error, including lack-of-fit and pure error

B_i, B_{ij}, B_{ijk} = unknown coefficients that must be estimated from the experimental data.

For a particular mixture, the pseudo-components G, Z, and W in Equation (1) are given by:

Glass Formers: $G = [(\text{wt\% glass formers}) - 70]/30$

ZrO_2: $Z = [(\text{wt\% } ZrO_2) - 0]/30 = (\text{wt\% } ZrO_2)/30$

Waste-ZrO_2: $W = [(\text{wt\% waste}) - 0]/30 = (\text{wt\% waste})/30$

where the wt% of each component is expressed as a percentage. Each pseudo-component is computed by subtracting the minimum wt% given in Table 5 from the wt% of the component in the mixture and then dividing the difference by the quantity 1 minus the sum of the minimum wt% values for the three components. Pseudo-components are used rather than the original component wt% values for computational reasons.

The set of mixtures was selected to include the four extreme vertexes, the four edge centroids, and the overall centroid of the mixtures region defined by the component ranges given in Table 5 and the constraint that the component proportions in a mixture must equal 1. Since there are seven unknown coefficients in Equation (1) and only nine mixtures that represent the experimental region, it was decided that all nine mixtures should be included in the

experiment and that three of them should be replicated (i.e., melted and tested twice) to provide an estimate of the experimental error variance. The nine distinct mixtures are displayed in Table 6, with the replicated mixtures indicated. The 12 mixtures were melted and tested in a completely random order.

TABLE 6. Set of Experimental Mixtures

Glass	Glass Composition, wt%			
	Glass Formers	ZrO_2	Waste-ZrO_2	
1(a)	85	15	0	Extreme Vertexes
2(a)	85	0	15	
3	70	15	15	
4(a)	70	0	30	
5	77.5	7.5	15	Overall Centroid
6	70	7.5	22.5	Edge Centroids
7	85	7.5	7.5	
8	77.5	0	22.5	
9	77.5	15	7.5	

(a) Two replicates of this glass were included.

ZrO_2 Variability Results

The results for each property are discussed separately in subsequent sections. However, this section presents some general information that is helpful in examining the results for each property.

An analysis of variance was conducted for the properties of interest in this study. Examples of the variance analysis as well as the modeling results are shown for T100P, E1150, and MCC-3 boron release in Tables 7, 8, and 9, respectively. In each table, the adjusted R-squared value indicates the fraction of variation in the property values that is accounted for by the fitted model. Generally, if a fitted model has an adjusted R-squared value of approximately 0.90 or larger and a nonsignificant lack-of-fit (LOF), the model is said to adequately characterize the property over the experimental region. Also, the results of a test for LOF are given. The LOF test compares the "average" of the squared deviations of the observed values from the fitted

TABLE 7. Analysis of Variance (ANOVA) and Modeling Results for T100P

Source of Variance	Analysis of Variance: Degrees of Freedom	Sum of Squares	Mean Square
Total	11	0.22866×10^5	
Regression	6	0.22426×10^5	0.37376×10^4
Error	5	0.44050×10^3	0.88100×10^2
LOF	2	0.31000×10^3	0.15500×10^3
Pure Error	3	0.13050×10^3	0.43500×10^2

Adjusted R-Squared = 0.9576

Lack of Fit F Test = F = 3.56, Not Significant

Pseudo-Component	Coefficient
G	1346.67121
Z	1216.35978
W	1151.41099
G x Z	-282.41807
G x W	-611.09833
Z x W	92.90186
G x Z x W	-215.99871

Glass	Predicted	Observed
8	1085.645	1089.000
2a	1096.267	1099.000
1a	1210.911	1202.000
9	1164.067	1172.000
3	1207.111	1202.000
4a	1151.411	1150.000
1b	1210.911	1217.000
4b	1151.411	1150.000
2b	1096.267	1093.000
7	1152.645	1156.000
6	1185.067	1193.000
5	1127.288	1116.000

TABLE 8. Analysis of Variance (ANOVA) and Modeling Results for E1150

Source of Variance	Analysis of Variance: Degrees of Freedom	Sum of Squares	Mean Square
Total	11	0.17466×10^{-1}	
Regression	6	0.17338×10^{-1}	0.28897×10^{-2}
Error	5	0.12749×10^{-3}	0.25499×10^{-4}
LOF	2	0.94494×10^{-4}	0.47247×10^{-4}
Pure Error	3	0.33000×10^{-4}	0.11000×10^{-4}

Adjusted R-Squared = 0.9839

Lack of Fit F Test = F = 4.30, Not Significant

Pseudo-Component	Coefficient
G	0.28810
Z	0.39403
W	0.26233
G x Z	-0.70494
G x W	-0.00706
Z x W	-0.48706
G x Z x W	0.95200

Glass	Predicted	Observed
8	0.267	0.271
2a	0.273	0.272
1a	0.165	0.168
9	0.215	0.218
3	0.206	0.205
4a	0.262	0.262
1b	0.165	0.160
4b	0.262	0.261
2b	0.273	0.273
7	0.218	0.222
6	0.204	0.207
5	0.226	0.219

TABLE 9. Analysis of Variance and Modeling Results for MCC-3 Boron Release

Source of Variance	Analysis of Variance: Degrees of Freedom	Sum of Squares	Mean Square
Total	11	0.16086×10^{2}	
Regression	6	0.15032×10^{2}	0.25053×10^{1}
Error	5	0.10540×10^{1}	0.21080×10^{0}
LOF	2	0.10040×10^{1}	0.50200×10^{0}
Pure Error	3	0.50000×10^{-1}	0.16667×10^{-1}

Adjusted R-Squared = 0.8559

Lack of Fit F Test = F = 30.12, Significant

Pseudo-Component	Coefficient
G	13.34207
Z	0.94455
W	0.54796
G x Z	-23.66143
G x W	-13.95262
Z x W	-1.39261
G x Z x W	15.20000

Glass	Predicted	Observed
8	1.130	0.600
2a	3.457	3.500
1a	1.228	1.300
9	0.416	0.370
3	0.398	0.300
4a	0.548	0.570
1b	1.228	1.300
4b	0.548	0.670
2b	3.457	3.800
7	2.730	2.200
6	0.386	0.340
5	0.924	1.500

model (LOF MS in each table) with the estimate of the experimental error variance (pure error MS in each table) by comparing the ratio F = (LOF MS)/(pure error MS) with a table value from the F-distribution with two and three degrees of freedom at a specified significance level. For this study, the 0.10 significance level was used; the table value is 5.46. If the F-ratio exceeds the table value, the LOF is statistically significant and indicates that the fitted model does not account for all of the nonrandom variations in the property data.

Tables 7 through 9 also display the estimates of the seven coefficients in Equation (1) for each of the fitted property models. The observed and predicted property values for the 12 experimental glasses illustrate how well the fitted models predict the property values. To illustrate the use of the fitted models to predict a property value, suppose that it is of interest to predict T100P at the centroid composition. The centroid composition has 77.5% glass formers, 7.5% ZrO_2, and 15% waste-ZrO_2. The pseudo-components are computed as:

$$G = (77.5 - 70)/30 = 0.25$$
$$Z = (7.5 - 0)/30 = 0.25$$
$$W = (15 - 0)/30 = 0.50$$

The coefficient estimates are found in Table 7, which also indicates which pseudo-components should be multiplied. Using the information from Table 5 together with the definition of Equation (1), the predicted value of T100P at the centroid composition is computed as:

$$\begin{aligned} T100P &= 1346.67121(0.25) + 1216.35978(0.25) + 1151.41099(0.50) \\ &\quad - 282.41807(0.25)(0.25) - 611.09833(0.25)(0.50) \\ &\quad + 92.90186(0.25)(0.50) - 215.99871(0.25)(0.25)(0.50) \\ &= 1127.3 \end{aligned}$$

The other properties are predicted in a similar manner.

Figures 6 through 8 (T100P, E1150, and MCC-3 boron) are examples of the contour plots of the predicted properties over the experimental region. The contour plots are constructed by simulating a "grid" of glass compositions within the experimental region. The fitted model for a particular property is

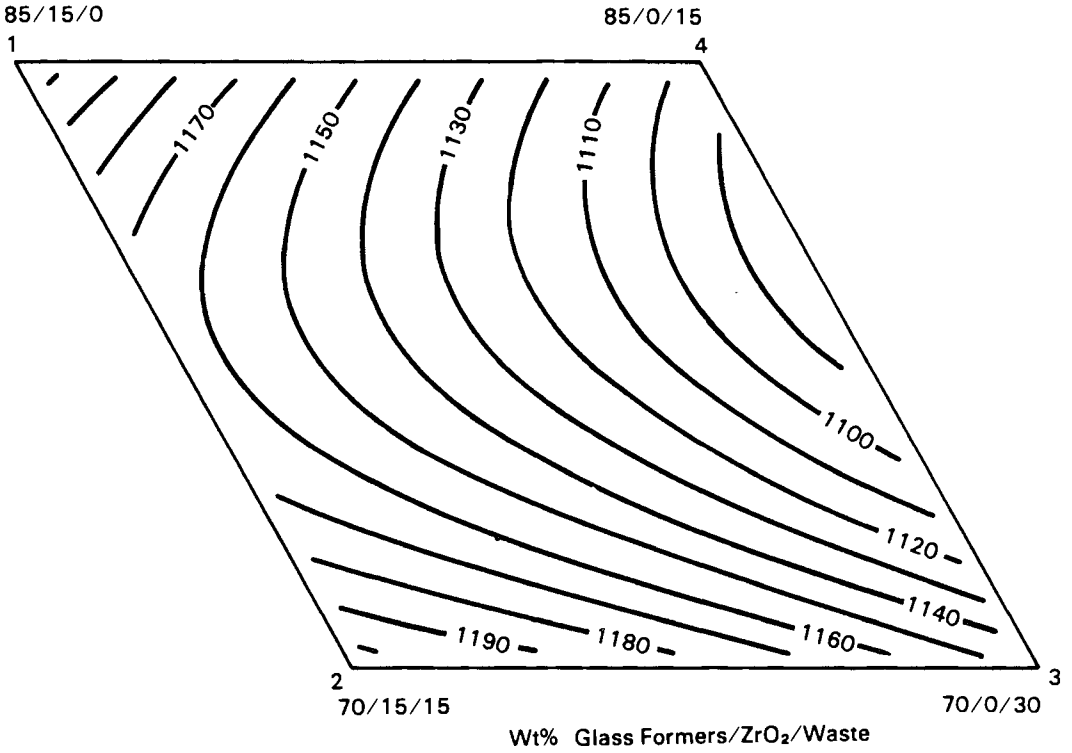

FIGURE 6. Contour Plot of Predicted 100 Poise Temperature (T100P)

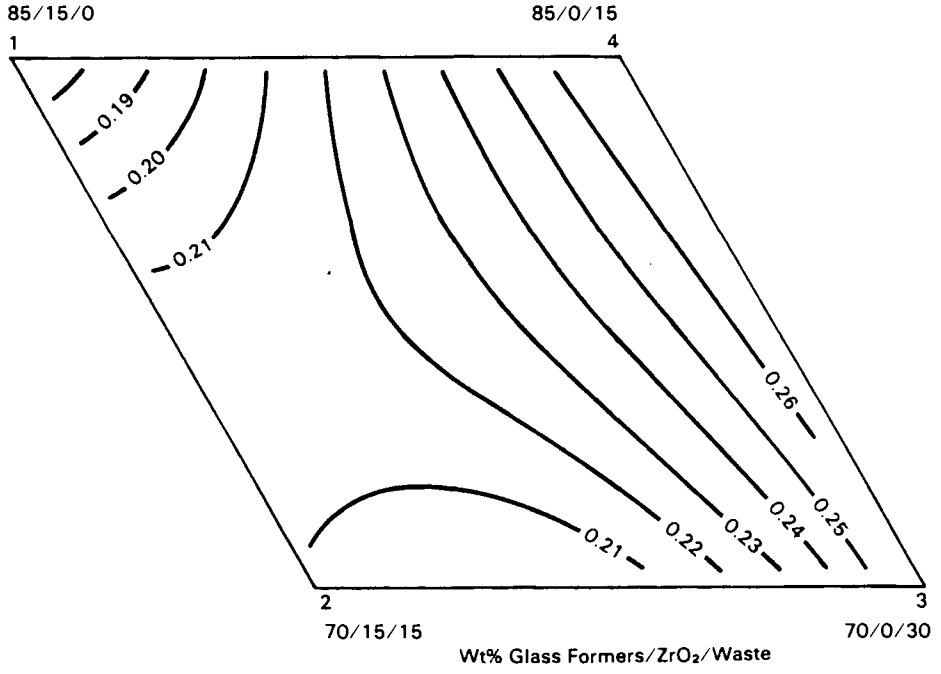

FIGURE 7. Contour Plot of Predicted Electrical Conductivity at 1150°C (E1150)

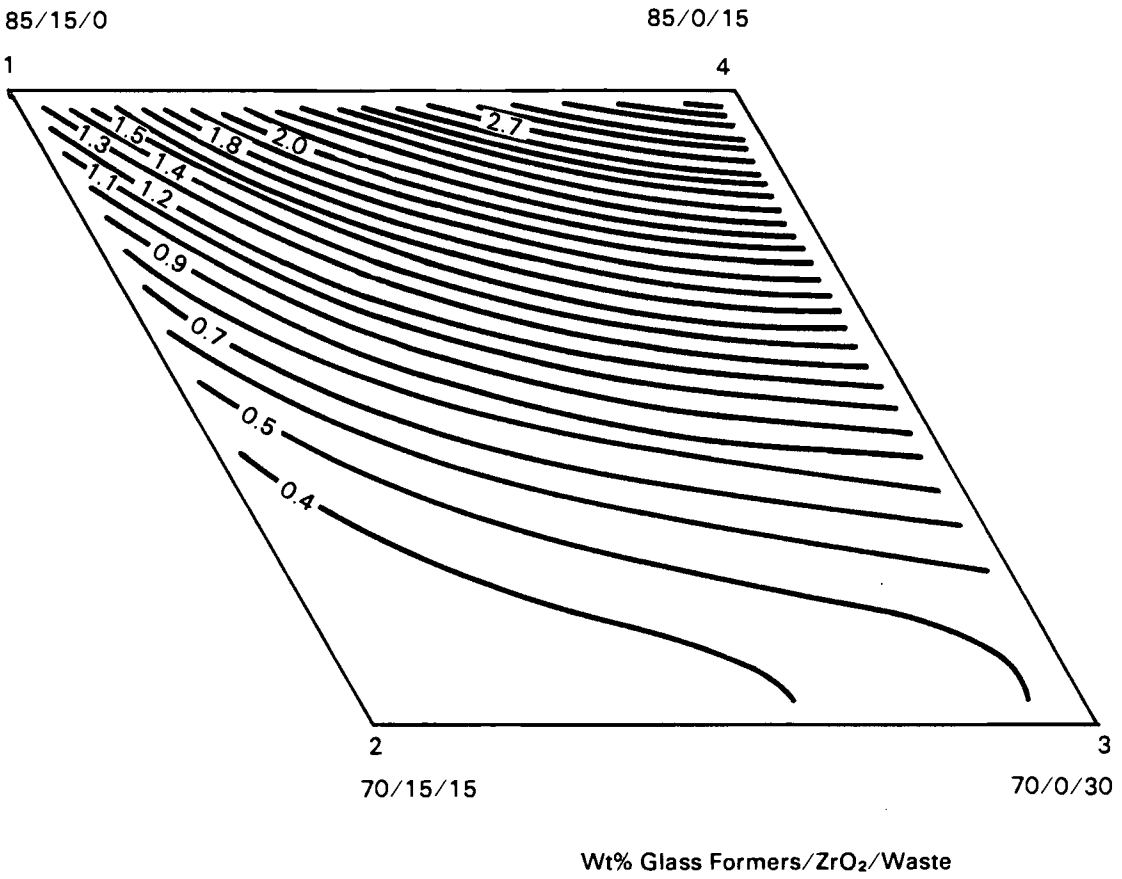

FIGURE 8. Contour Plot of Predicted Normalized Release for Boron from MCC-1 Testing (28-day, 90°C, SA/V = 10 m^{-1})

then used to predict property values for each composition on the grid. The resulting predicted values are plotted at specific increments as contours over the experimental region. To aid in interpreting the contour plots, the vertexes of the experimental region are numbered. The numbered vertexes (e.g., see Figure 6) correspond to the compositions (in wt%) listed in Table 10.

TABLE 10. Compositions at Vertexes on Contour Plots

	Glass Composition, wt%		
Vertex	Glass Formers	ZrO_2	Waste-ZrO_2
1	85	15	0
2	70	15	15
3	70	0	30
4	85	0	

Referring to Figure 6 and the definitions of the numbered vertexes in Table 10, the edge connecting Vertexes 1 and 4, henceforth called the (1,4) edge, is the upper limit on wt% glass formers, and the (2,3) edge is the lower limit on wt% glass formers. Moving along any imaginary vertical line that is perpendicular to the (2,3) edge, and the (1,4) edge, corresponds to changes in wt% glass formers. Moving along or parallel to an imaginary line connecting Vertex 2 with the midpoint of the (3,4) edge corresponds to changes in wt% ZrO_2; moving from the lower left to the upper right corresponds to decreasing wt% ZrO_2. Moving along or parallel to an imaginary line that connects Vertexes 1 and 3 corresponds to changes in wt% waste-ZrO_2; moving from the upper left to the lower right corresponds to increasing wt% waste.

Viscosity Results at T100P

The T100P modeling results are displayed in Table 7. The fitted model has an adjusted R-squared value of 0.96 and a nonsignificant LOF. Thus, the fitted model should be quite reliable for predicting the major trends in T100P as the three components are varied over the experimental region.

The quantity of glass formers has a strong negative effect as it is increased from its lower limit to the centroid composition; then, from the centroid composition to the upper limit, the negative effect weakens and becomes positive. ZrO_2 has a strong positive effect. The wt% of the waste has a strong negative effect as it is increased from its lower limit to the centroid composition; then, as wt% waste increases from the centroid composition to its upper limit, the negative effect weakens and becomes positive.

Figure 6 is the contour plot of predicted T100P. The minimum predicted T100P occurs along the (3,4) edge about two thirds of the way from Vertex 3 to Vertex 4. The steepest increase in predicted T100P is achieved by moving from the minimum point towards either Vertex 1 or Vertex 2. The minimum increase is achieved by moving from the minimum towards the midpoint of the (1,2) edge.

For melter operation, the temperature at which the glass has a viscosity of 100 poise (T100P) should be between 1070°C and 1150°C. If the T100P is outside this range, processing problems may be encountered in the melter. Assuming a 25 wt% total waste loading (ZrO_2 + waste) and using the model to

evaluate the T100P, it is predicted that the glass could contain up to 10 wt% ZrO_2 (40 wt% in the waste) before the T100P of the glass exceeds 1150°C. The total waste loading of the glass would need to exceed 30 wt%, with the current ZrO_2 concentration of 0.6 wt%, before a T100P of 1150°C is reached.

Electrical Conductivity Results at E1150

The E1150 modeling results are displayed in Table 8. The fitted model has an adjusted R-squared value of 0.98 and a nonsignificant LOF. Thus, the fitted model should be quite reliable for predicting the major trends in E1150 as the three components are varied over the experimental region.

The amounts of glass formers and waste both have strong positive effects. ZrO_2 has a strong negative effect as it is increased from its lower limit to the centroid composition. As it is increased from the centroid composition to its upper limit, the negative effect weakens.

Figure 7 is the contour plot of predicted E1150. The maximum predicted E1150 values occur approximately along the (3,4) edge. The steepest decrease in predicted E1150 is achieved by moving from Vertex 4 to Vertex 1 or from Vertex 3 to Vertex 2. The minimum decrease is achieved by moving from any point along the (3,4) edge to approximately the midpoint of the (1,2) edge. Typically in joule-heated ceramic melters, the electrical conductivity of the glass melt should be 0.18 to 0.5 $(ohm\text{-}cm)^{-1}$ at 1150°C. As can be seen on the contour plots and confirmed using the model, the electrical conductivity of the glass does not exceed the range recommended for melter operation over the ranges of compositions tested. Within the more restrictive composition range required to produce an acceptable T100P, the E1150 of the glass melt is well within the required range.

Summary of Leaching Results

The major trend in all the leaching results is that as the ZrO_2 increases from 0 to 15 wt% in the glass the durability of the glass also increases. The HWVP reference glass composition has 0.6 wt% ZrO_2; thus, any increase in ZrO_2 content due to waste variability will produce an acceptable glass from the standpoint of durability.

Changes in the waste loading of the glasses can have both positive and negative effects on the durability. However, over the range of waste loadings most likely to be used (20 to 30 wt%), changes in the elemental release rates are not sufficient to disqualify the glass.

A visual examination of the effects plots and contour plots reveals that the predicted B, Na, and Si releases from the MCC-3 test behave almost identically when the three components are varied over the experimental region. The actual predicted values of the three quantities are different, but the trends that show up in the plots are very nearly the same. The Ca and Cs releases also follow the same basic trends observed in the B, Na, and Si plots. Similarly, the predicted releases from the MCC-1 test behave almost identically in response to changes in the three components. Also, comparing the effects and contour plots for release rates from both the MCC-1 and MCC-3 tests reveals that the maximum predicted values occur near Vertex 4 and the minimum values occur in the lower left region of the plot for B, Na, Si, Ca, and Cs.

Because the same basic trend is observed in the release data, only the data for MCC-3 boron release is shown here as an example (see Table 9). The fitted model has an adjusted R-squared value of 0.86 and a statistically significant LOF. However, with an adjusted R-squared of 0.86, the model should be quite useful for predicting some major trends in B release as the three components are varied over the experimental region.

Glass formers have a strong positive effect; increasing the wt% glass formers causes an increase in the predicted B release. ZrO_2 and waste both have negative effects; increasing wt% ZrO_2 or wt% waste decreases the predicted B release.

Figure 8 is the contour plot of MCC-3 B release. The maximum predicted B release values occur near Vertex 4. The steepest rate of decrease in predicted B release results from decreasing wt% glass formers while increasing wt% ZrO_2 (i.e., moving from Vertex 4 towards Vertex 2).

Concluding Remarks for ZrO_2 Variability

To illustrate the utility of the fitted models and their corresponding plots, suppose that it is of interest to minimize elemental release, but the

process requires that the T100P must not exceed 1150°C. Figure 6 can be used to identify the range of glass compositions in the experimental region where the predicted T100P does not exceed 1150°C. In fact, the region to the right of the 1150 contour in Figure 6 defines all glass compositions in the experimental region that have predicted T100P values less than 1150°C. This constrains the minimization of elemental release because compositions in the lower left portion of the plot, where the minimum predicted elemental release values occur, have predicted T100P values that exceed 1150°C. The lowest predicted elemental release values among compositions with acceptable predicted T100P values occur along the 1150 contour, in the vicinity of its intersection with an imaginary line connecting Vertexes 2 and 4. In fact, if Figure 6 is overlaid on any of the contour plots for MCC-1 or MCC-3 B, Na, or Si release, a small region is easily identified where elemental release is approximately minimized, subject to the requirement that T100P must not exceed 1150°C. This region can be examined on the plots of predicted Ca and Cs release and the plot of predicted E1150 to determine whether any further restrictions apply.

CONCLUSIONS

The following conclusions can be drawn from the work conducted this quarter:

- Simulated HWVP melter feeds, prepared by treating with formic acid and adding frit, gelled when allowed to stand undisturbed. The gel prevents the frit and insoluble waste particles from settling to the bottom of the feed.
- Melter feeds prepared using aged simulated HWVP feed exhibited some dilatant fluid behavior at concentrations of 500 g TO/L or higher.
- Boiling the melter feed had little effect on the yield stress and apparent viscosity at concentrations below 550 g TO/L but had an effect at concentrations of 600 g TO/L.
- Boiling had an effect on the melter feed pH, but rheological properties do not appear to be a function of pH in the range studied except at a concentration of 600 g TO/L.

- Assuming a 25 wt% total waste loading (ZrO_2 + waste) and using the model to evaluate the T100P, it is predicted that the glass could contain up to 10 wt% ZrO_2 (40 wt% in the waste) before the T100P of the glass exceeds 1150°C, which is the upper limit for melter operation. If all the ZrO_2 is removed from the glass, a T100P of approximately 1100°C is predicted.
- The electrical conductivity of the glass does not exceed the range recommended for melter operation over the ranges of compositions tested. Within the more restrictive composition range required to produce an acceptable T100P, the E1150 of the glass melt is well within the required range.
- The addition of ZrO_2 to the glass over the range tested increased the durability of the glass.
- In glasses with 20 to 30 wt% waste loading, the release rates for B, Ca, Na, Si, and Cs are similar to the release rates of the reference glass, HW39.

REFERENCES

Burkholder, H. C., J. H. Jarrett, and J. E. Minor, Compilers. 1986. LFCM Vitrification Technology, Quarterly Progress Report, July-September 1985. PNL-5470-4, Pacific Northwest Laboratory, Richland, Washington.

FEED PREPARATION AND TRANSFER SYSTEMS

M. E. Peterson and R. K. Nakaoka

SUMMARY

A detailed test procedure was prepared to characterize and evaluate the resuspension of melter feed slurries in pipes. The testing will involve characterizing the physical properties of the solid and liquid phases of the slurry, the piping system using Newtonian fluids, the piping system using fully suspended slurry, and the slurry flow over a sediment bed.

INTRODUCTION

Feed preparation and transfer systems consist of the equipment used to contain and process liquid high-level waste (HLW) between the point of entry into a vitrification facility and the melter chamber. The equipment includes tanks, concentrators, agitators, pumps, process monitors, transfer lines, and the cooled melter feed nozzle. These systems also include the equipment used to batch the glass-forming additives and to convey them into the feed makeup tank for blending with liquid HLW.

Activities and results of the work being performed at Pacific Northwest Laboratory (PNL) to support the development, design, selection, and operation of the feed preparation and transfer systems are discussed. During FY 1986, specific activities concerning feed preparation and transfer systems include:

- evaluation of the resuspension of simulated melter feed slurries in pipes
- bench-scale testing to determine the design of heat transfer equipment (jacket or coils) for the slurry feed makeup tanks
- selection of the sampler, level detector, and transfer pump for the full-scale mixing tank

- radioactive demonstration of melter feed transfer equipment in support of radioactive demonstration of the liquid-fed ceramic melter (LFCM)
- installation and functional testing of a full-scale melter feed slurry mixing tank complete with agitator and proper impellers.

TECHNICAL PROGRESS

Experience with melter feeds at PNL has shown that slurries have a tendency to settle and form deposits that are difficult to resuspend. This settling of solids may occur in transfer lines and processing equipment. A comprehensive collection of the literature concerned with the resuspension of settled solids was completed and reviewed. This literature review was used to define the experimental objectives and procedures.

The objective of the resuspension experiments will be to characterize the resuspension of a simulated melter feed slurry in pipes as a function of the average slurry velocity over a sediment bed. Theoretical and experimental parameters must be considered.

Melter slurry consists of an exceptional number of diverse components. Slurry behavior under settling conditions is assumed to be a basic dewatering process resulting in two distinctive phases. The lighter layer consists primarily of water. The second layer is a multicomponent sludge that will be classified as a sediment bed.

Previous work in the field of solid/liquid transport suggests that once a stationary bed of solids has been formed the controlling parameter in the redistribution of particles into the liquid stream is the flow-induced shear stress at the bed surface. Motion of a solid particle off the bed will occur only if the effects of gravity and particle/particle interactions are overcome by forces imparted by the flowing liquid. The bed shear stress can be translated into a bed velocity and then related to an average bulk velocity.

Theoretically, the physical characteristics of the liquid stream and solid particles can be incorporated into a hydrodynamical force balance and then the

critical liquid velocity needed for resuspension can be determined. For the majority of systems, it is difficult to define the physical properties of the system to the extent of achieving a valid theoretical solution. Important parameters in the theoretical solution include particle size distribution, mean particle density, shape factors, fluid density, fluid viscosity, and zeta potential. These parameters are used to determine drag and lift coefficients used in the force balance.

Fluid flow through a pipeline has been well defined in the literature for a Newtonian fluid in the laminar flow region. Melter slurry is more closely approximated using a yield-pseudoplastic model with a relatively small value for yield stress. In some cases, a pseudoplastic model can be used without generating appreciable error.

Measurements of flow parameters in pipes are generally limited to average or bulk values. It becomes very difficult to experimentally measure local values of such things as velocity or shear stress. Thus, a comparison of theoretical and experimental bed velocities at incipient motion is not usually obtainable.

Because of the difficulties in measuring local values of flow parameters, it becomes more efficient to track average or bulk properties of pipe flow. The problem then becomes one of translating bulk values to local values using either theoretical or empirical relationships. Many times, the more-established formulas apply only to Newtonian fluids; little work has been done with non-Newtonian fluids.

One of the easiest parameters to measure in pipe flow is pressure drop over a specific length of pipe. By varying the bulk fluid velocity and measuring the corresponding pressure drop, a number of relationships can be established for a particular fluid and piping system.

In studying the resuspension of solids in a flowing liquid media, the quantities of interest are the bulk fluid velocity that initiates incipient motion (beginning of bed movement), the corresponding bed velocity and shear stress, the bulk fluid velocity when the last of the sediment bed has been removed, and the relationship between bulk fluid velocity and head loss.

The experimental procedures used in the evaluation of melter feed slurries can be divided into four parts: characterization of the solid/liquid system, characterization of the piping system, characterization of fully suspended slurry flow, and characterization of slurry flow over a sediment bed.

CHARACTERIZATION OF THE SOLID/LIQUID SYSTEM

To resuspend melter slurry that has settled to the bottom of a pipe, it is necessary to define the system consistently. The dense sludge layer that has been deposited on the floor of the pipe will be designated as the solid phase of the system. The physical properties of a settled sludge were not investigated prior to this test. Important properties include composition, apparent viscosity, temperature dependence of apparent viscosity, density, pH, dissolved solids, suspended solids, total solids, particle size distribution, mean shape factor and settling rate.

To understand the complexibility of the system, certain characteristics of the liquid and solids layers must be determined. Important parameters include composition and density.

CHARACTERIZATION OF THE PIPING SYSTEM

The piping system specified for this test includes two mixing tanks (with agitators), a 10- to 30-ft section of straight pipe with three different pipe diameters, a 10- to 15-ft test section of clear PVC pipe, a manometer to measure pressure drop over the test section, and a progressive-cavity positive-displacement pump.

The first step of the experimental procedure will be to verify the behavior of the piping system using an easily characterized Newtonian fluid and well-established relationships. Water, selected as the Newtonian fluid, will run through the pipe system at progressively higher velocities, and the pressure drop across the clear PVC test section will be recorded. By plotting the shear stress ($D\ \Delta P/4L$) versus the shear rate ($8V/D$) on a log-log scale, the validity of the Metzner and Reed (M-R) equation, Equation (1), can be assessed.

$$D\ \Delta P/4L = K' (8V/D)^n \quad (1)$$

where D = inside diameter of the pipe, ft
ΔP = pressure drop, lb/ft^2
L = equivalent length, ft
K′ = consistency index, $lb\text{-}s/ft^2$
V = average velocity in pipe, ft/s
n = flow behavior index.

For a Newtonian fluid, n = 1 and K′ should be equal to the viscosity. The flow behavior index (n) is equal to the slope of the log-log plot described above, and the consistency index is the intercept of the plot with the line at a shear rate of 1/s. The flow transition from laminar to turbulent can be seen from the sample graph. The point at which the slope of the best-fit straight line sharply increases corresponds to the laminar/turbulent transition velocity, which can be related to a transition Reynolds number (Re).

The relationship between pressure drop and water velocity can also be used to establish the roughness of the test section. Equation (2) applies to Newtonian fluids and relates pressure drop and velocity to friction factors. Using a standard Moody plot and values of Fanning friction factor and Re in the turbulent region of flow, a roughness factor for the test section of the system can be determined.

$$f = \frac{D\Delta P}{4L} \Big/ \frac{\rho V^2}{2g} \quad (2)$$

where f = Fanning friction factor
D = diameter of inside pipe, ft
ΔP = pressure drop, lb/ft^2
L = equivalent length, ft
V = average fluid velocity, ft/s
ρ = fluid density, lb/ft^3.

A plot of friction factor versus Re (log-log) for water in our system should yield the following relationships:

$$\text{laminar region } f = 16/Re \tag{3}$$

$$\text{turbulent region } f = 0.0791\ Re^{-1/4} \tag{4}$$

The Re that corresponds to the transition of laminar to turbulent flow should be easily determined from the graph.

CHARACTERIZATION OF FULLY SUSPENDED SLURRY FLOW

The behavior of fully suspended (no sediment bed) melter slurry in the piping system should be established. Because a low velocity may lead to deposition of solid particles, this test should start with high fluid velocities and the velocity should be gradually reduced. The pressure drop across the test section will be measured for each velocity as before. Equation (1) applies and a plot of $D\ \Delta P/4L$ versus $8V/D$ on a log-log scale will yield values for the flow behavior index, n, and the consistency index, K'.

Because melter slurry is a non-Newtonian fluid, the relationship between pressure drop and friction factor described in Equation (2) does not apply. The equations listed below are valid for pseudoplastic fluids. The values for n and K' are determined as described above.

Since the yield stress exhibited by melter slurry is small, the assumption of pseudoplastic behavior will be tested by plotting f versus Re(M-R). If the experimental friction factors reasonably fit Equations (5) and (6), the treatment of melter slurry as a pseudoplastic is valid. If not, the relationships formulated for a yield-pseudoplastic fluid will need to be used.

For pseudoplastic fluids:

Laminar Region

$$f = \frac{16\ \gamma}{D^n V^{2-n} \rho} \tag{5}$$

where $\gamma = 8g_c K'$

D = inside diameter of pipe, ft

V = average velocity of fluid, ft/s

ρ = density of fluid, lb/ft^3

n = flow behavior index

K' = consistency index, $lb\text{-}s/ft^2$.

Turbulent Region

$$\frac{1}{f^{0.5}} = \frac{4.0}{n^{0.75}} \log Re(M\text{-}R)\, f^{(1-n/2)} - \frac{0.40}{n^{1.2}} \tag{6}$$

Reynolds number, Re(M-R)

$$Re(M\text{-}R) = \frac{D^n V^{2-n} \rho}{\gamma} \tag{7}$$

Again, from the plot of f versus Re(M-R), the transition from laminar to turbulent flow can be determined.

Yield-pseudoplastic fluids differ from pseudoplastic fluids in that they exhibit a yield stress (the stress that must be exceeded in order for flow to begin). Yield stress alters the velocity distribution patterns developed during laminar flow. A higher shear rate is required to achieve a given velocity distribution pattern as opposed to a fluid without a yield stress. This additional shear rate requirement produces a higher value of Fanning friction factor at a given laminar Re. In addition, the transition Re (laminar to turbulent) is increased.

CHARACTERIZATION OF SLURRY FLOW OVER A SEDIMENT BED

The main objective of this investigation is to characterize the behavior of slurry flow in a pipe in the presence of a sediment bed. The sediment in this case is a sludge layer (dewatered slurry) that results when slurry is allowed to stand in a pipe line for a designated amount of time. Once the

sediment bed is established, fully suspended slurry will be pumped across the bed with increasing velocities. For each value of velocity, a pressure drop across the test section of the system will be determined. The fluid velocity will be increased until the entire sludge layer is removed. Figure 1 shows typical curves that will be constructed for pressure drop versus fluid velocity.

In the left-hand graph, there are three major points of interest: Point A corresponds to the incipient motion velocity; Point B represents the maximum pressure needed to establish heterogeneous flow; and Point C is the start of fully suspended flow.

In the right-hand graph, a change in slope signifies a change in flow characteristics. Point A is designated as the critical point for incipient motion and Point B signals the onset of fully suspended flow.

Using the two relationships illustrated in Figure 1, the values obtained for incipient motion velocity and velocity at which fully suspended flow is maintained can be compared.

As stated above, the physical force that induces particle resuspension is shear stress at the surface of the bed. In this study, critical shear stress can be determined from the value of the total friction factor at the critical fluid velocity. The friction factor associated with incipient motion is equal to the slope of the first line in the graph of head loss per unit length versus V/8gR and is based on Equation (8).

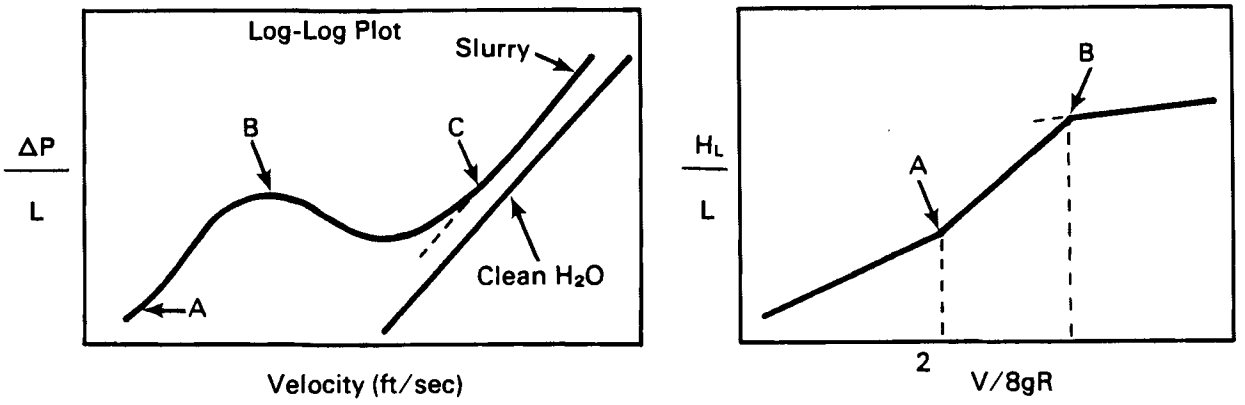

FIGURE 1. Velocity Versus Pressure

$$H_L/L = f_1 \frac{L_1}{L} + \frac{L_2}{L} \frac{V^2}{8gR} \quad (8)$$

The slope of the line (total friction factor) is equal to a sum of two friction factors. The first is due to contact with the sediment bed; the second is due to contact with the pipe wall. This second quantity was established in the experiment with fully suspended slurry. It is assumed that the viscous shearing forces are uniform over the entire surface of contact. By solving Equation (8), f_1 can be determined (assuming bed depth and pipe geometry are known). Equation (9) is then used to calculate the shear stress needed at the surface of the sediment bed to induce particle movement:

$$f = \frac{8gR\ \tau_1}{\rho V^2} \quad (9)$$

where g = gravitational constant, lb-ft/lb-s
R = hydraulic radius
τ_1 = shear stress, lb/ft^2
ρ = fluid density, lb/ft^3
V = fluid velocity, ft/s.

Critical shear stress and bed velocity have been studied for open channel-stream flow situations in the past. The Shields diagram is the most widely established relationship between bed shear stress and velocity. Once values are obtained for slurry resuspension, a comparison can then be made with values for simpler classical systems, such as sand and water in an open channel flow.

Another possibility for comparison of data would be the application of theoretical equations to the melter slurry system. Theoretical relationships are usually based on simplified or easily characterized systems. Physical properties of melter slurry determined by different methods could be incorporated in hydrodynamical force balance models presented by Kao, Wood, and LaBoon (1978) and values for critical velocity could be determined and compared with experimental values. Based on the agreement or disagreement between theory and experiment, some insight into the physical interactions of the system could be

obtained. A simplified model may be sufficient to approximate melter slurry behavior; but additional assumptions will probably be needed to adequately predict resuspension velocities for slurries.

Each of the steps outlined above should be conducted for every pipe diameter under consideration. This test procedure will effectively characterize the resuspension of melter feed slurries in pipes. The knowledge gained from these experiments can then be applied to the resuspension in other types of process equipment.

CONCLUSIONS

The following conclusion is based on the work described in the preceding sections:

- The prepared test procedure should effectively characterize the resuspension of simulated melter feed slurries.

REFERENCES

Kao, D. T., D. J. Wood, and J. H. LaBoon. 1978. Sediment Resuspension in Slurry Pipelines. IMMR36-RRR3-78, Prepared for the Institute for Mining and Materials Institute, College of Engineering, University of Kentucky, Lexington.

MELTER SYSTEMS

J. M. Perez, Jr., R. D. Dierks, and R. W. Goles

SUMMARY

Activities of the radioactive liquid-fed ceramic melter (RLFCM) vitrification system were directed towards preparations for operation in the second quarter of FY 1986. Therefore, there are no reportable activities for this report.

The nonradioactive pilot-scale ceramic melter (PSCM) was operated for 18 days in the fourth quarter of FY 1985 and produced a considerable amount of data. Operational data were presented in the previous quarterly report. Off-gas data analyzed in the first quarter of FY 1986 presented here are also presented in the off-gas systems section. The work was conducted under the Hanford Waste Vitrification Program in support of the glass waste form and melter feed slurry development.

INTRODUCTION

The objective of this work is to demonstrate laboratory-developed melter concepts, first with simulated radioactive feeds in the engineering-scale ceramic melters, then in the nonradioactive PSCM, and finally with radioactive feed compositions in the pilot-scale RLFCM. The laboratory-developed concepts include feed formulation modifications that affect melter performance (foaming, slag formation, free metal precipitation, scum formation) or the final glass characteristics (crack formation, leachability, devitrification).

An additional objective of this work is to evaluate melter facility process equipment modifications, first with simulated radioactive feeds in the PSCM, and then with radioactive feeds in the RLFCM. The process equipment modifications include feed tank agitation, slurry sampling, glass sampling, feed delivery systems, off-gas treatment systems, process variable sensor development, and process control concepts.

TECHNICAL PROGRESS

Progress on nonradioactive testing conducted this quarter is discussed below.

NONRADIOACTIVE TESTING

Process development work in FY 1985 concentrated on the development of reference glass and melter slurry compositions. The reference waste composition to be incorporated into a borosilicate glass matrix was a blend of two waste types: 1) the first-cycle extraction waste from the plutonium and uranium extraction (PUREX) process (neutralized current acid waste or NCAW) and 2) the transuranic (TRU) waste fraction of the cladding removal waste (CRW) stream. Extensive laboratory work was conducted to develop candidate glass and slurry compositions with acceptable physical and chemical properties. Based on laboratory results, an initial reference glass and two candidate feed slurries were recommended for LFCM testing. Two melter experiments were conducted in FY 1985. The first experiment was an engineering-scale test in the high-bay ceramic melter (HBCM). This experiment established the processability of the slurry composition. From this it was concluded that higher processing rates were possible using frit as the glass-forming fraction rather than using unreacted chemical salts (Burkholder, Jarrett, and, Minor 1986a).

Based on the results of the HBCM experiment an 18-day PSCM experiment was conducted. The processing results were reported in Burkholder, Jarrett, and Minor (1986b). In the first quarter of FY 1986, the off-gas data analysis was completed. The results are reported in the following sections.

System Description

The PSCM and associated support equipment are shown in Figure 1. The glass tank has an exposed glass surface of 0.73 m^2 (almost one-third-scale of the current HWVP melter design). The melt tank is rectangular (69 cm wide by 104 cm from one electrode face to the other electrode face). At a normal glass overflow depth of 37 cm, the melt volume is 270 L. The electrodes are single 5-cm-thick Inconel 690 plates with 5-cm-thick "feet" that extend 13 cm into the

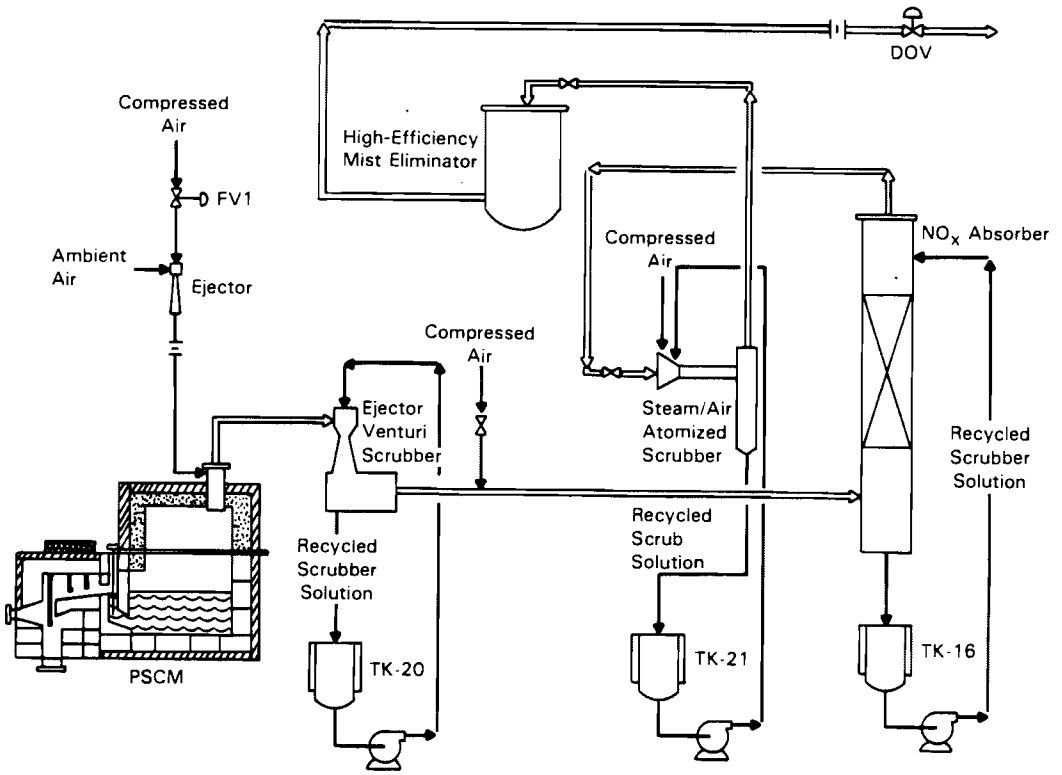

FIGURE 1. PSCM and Associated Off-Gas Treatment Equipment

melt. The feet cause the electrical current flux to be skewed slightly towards the floor of the melt tank. The additional heating keeps the floor area temperature comparable to the bulk glass temperature, which helps prevent spinel sludge formation.

The glass is discharged from the tank through a 7.6-cm riser port located near the melter floor in the center of the refractory wall. Glass can be discharged continuously from the melter or in batches via an air lift bubbler. Glass flows from the riser, down the discharge trough, and off the face block. The glass product is received in either 55-gal drums or instrumented canisters. The overflow discharge section is maintained at 1000 to 1100°C by six spiral bayonet-type silicon carbide heating elements.

The plenum space vacuum is maintained at 10 to 15 cm WC (water column) by the off-gas system. This system consists of a film cooler, located in the melter off-gas lid nozzle, ejector venturi scrubber (EVS), packed-column steam-atomized scrubber (SAS), and a high-efficiency mist eliminator (HEME). The operation of these systems is described in Scott, Goles, and Peters (1985).

Off-Gas System Performance

Effluent sampling was conducted to characterize volatile and particulate releases from the PSCM and the scrubbing efficiencies of the off-gas equipment. Operational off-gas performance characteristics of the EVS and HEME were obtained throughout the experiment as were melter effluent emission characteristics. The performance of the SAS was evaluated during the last two days of testing. However, when not operating, the off-gas stream still passed through the SAS. The HEME was operated with and without a co-current water spray wash.

Feeds containing the formate anion can produce significant concentrations of H_2 and CO. Previous PNL melter tests involving the feeds formated at Savannah River Laboratory (SRL) have shown relative production rates of CO_2, H_2, and CO to be 1, 0.5, and 0.1, respectively (Goles and Sevigny 1983). The relative production rates of CO_2, H_2, and CO observed during this experiment were 1, 0.1, and less than 0.1, respectively. The presence of highly oxidizing NO_x gases in the melter exhaust may have been responsible for reducing the net off-gas yield of hydrogen produced.

Melter gas-phase losses to the off-gas system were significant only for B, C, N, S, and the halogens, which all readily form volatile acidic gases. This is consistent with previous testing (Goles and Sevigny 1983). The presence of sugar had no effect upon volatility in the melter. The halogen feed components had the ability to penetrate all off-gas processing equipment studied.

Since effluent gas-phase losses were limited to B, C, N, S, and the halogens, most melter off-gas system losses were associated with aerosol emission. Off-gas equipment performance can be measured in terms of decontamination factors (DFs): the ratio of the mass rate of a component exiting a device to the mass rate of that component entering the device. Therefore, the larger the DF, the more efficient the device. The average feed component DFs established for the melter, EVS, HEME, and the SAS throughout the experiment are summarized in Table 1.

The melter performance in terms of DF was quite consistent and reasonable. The very low Cs DF is associated with the presence of formate anion and

TABLE 1. Average Elemental Decontamination Factors for the Melter and Off-Gas System

Element	Melter	EVS	HEME	SAS
Al	750.0	32.0	10.0	4.5
B	63.0	11.0	7.5	6.2
Ba	190.0	290.0	8.7	7.3
Ca	730.0	160.0	3.0	5.9
Ce	450.0	--	--	--
Cl	1.3	6.2	14.0	4.9
Cr	180.0	14.0	16.0	5.3
Cs	14.0	1.4	19.0	4.3
Cu	250.0	7.2	16.0	7.3
F	3.2	14.0	6.1	3.5
Fe	260.0	92.0	44.0	6.1
I	1.3	--	--	--
La	620.0	440.0	--	--
Li	500.0	2.6	19.0	5.0
Mg	630.0	94.0	1.0	1.2
Mn	300.0	220.0	36.0	5.5
Mo	57.0	1.6	19.0	4.8
Na	260.0	2.1	17.0	5.0
Nd	290.0	190.0	--	--
Ni	2100.0	3.7	64.0	6.1
Ru	42.0	1.4	32.0	4.8
S	1.8	4.3	18.0	2.3
Si	780.0	59.0	--	1.1
Sr	230.0	260.0	6.2	11.0
Ti	250.0	970.0	41.0	18.0
Zn	160.0	19.0	3.9	1.4
Zr	420.0	670.0	25.0	8.8
Total	180.0	5.0	5.6	1.7

is strikingly similar to previous PSCM data obtained during the processing of SRL-formated feeds (Goles and Sevigny 1983). Formated feeds appear to be exceptionally effective in promoting the Cs volatilization/condensation process in the melter plenum. As a result, they have been responsible for the lowest recorded melter Cs DFs measured at PNL. It should be noted that the sugar component of the feed has no apparent influence on Cs or overall melter losses.

Like the halogens, sulfur exhibited a very low average melter DF of 1.8. The additional formic acid added with the frit addition (3 g/L of melter feed) must have been responsible for promoting high volatile loss rates of sulfur.

The total melter DF for Ru was determined only during one day when it was added directly to the melter feed tank. Its relatively low DF of 42 is indicative of an initial volatilization mechanism; however, its subsequent conversion to an aerosol was quite prompt because all detected Ru melter off-gas system emissions were confined to the aerosol sample fraction.

The performance of the EVS was quite predictable. This scrubber is a low-efficiency device that is designed to deal only with large-diameter aerosols. As a result, EVS elemental DFs should be direct measures of the mass mean diameters of the aerosols responsible for individual feed component losses. The low aerosol DFs are probably attributable to the fact that a film cooler device was used upstream of the EVS. Because the film cooler used a noncondensable gas (air) as a sweep gas, a large process effluent dilution resulted upstream of the EVS, thus reducing contact and scrubbing efficiency. Steam collapse of the off gas during EVS quenching was also significantly reduced or eliminated by film cooler operations that may have contributed to the poor performance.

Because most aerosols penetrating the EVS are submicron, they all exhibited essentially the same HEME DFs. Effluents with volatilized components exhibited lower-than-average DFs. The variability associated with the HEME results in a reflection of analytical uncertainties at or near detection limits. The Cs DFs recorded during this experiment were a factor of about three higher than those observed during previous PSCM testing. These DFs, however, remain a factor of three below HEME design expectations. The reason for deficient performance may involve solution breaching of the filter element. Use of a water spray at the HEME inlet did not impact the HEME DFs. However, the mist carryover from the packed tower probably introduced as much moisture as did the 16-mL/min water spray when used. Only dry operation of the HEME has been successful in producing acceptable HEME performance (DF = 50) at PNL (Scott, Goles, and Peters 1985).

Most of the SAS elemental DFs observed during the experiment were lower than the values recorded for the HEME. Moreover, the DFs observed are not strongly element-dependent, which suggests that most aerosols penetrating the EVS are submicron. The single-stage Cs DFs observed during the experiment were

an order of magnitude lower than design values of 50 for a dual-cascade SAS system (Randall 1982). If it is assumed that the combined DFs associated with cascaded SASs are the square of single-stage performance, the Cs DF for this test would have been ~20, which is significantly less than that recorded at SRL (1983).

CONCLUSIONS

The performance of off-gas characterization and treatment equipment was assessed during the first PSCM experiment with the initial reference waste and melter feed compositions. Results of off-gas characterization are consistent with previous experiments in which a melter feed pretreated with formic acid was processed. Off-gas equipment performance was also consistent with past results. However, the efficiencies of the high-efficiency scrubber were below design expectations.

REFERENCES

Burkholder, H. C., J. H. Jarrett, and J. E. Minor, compilers. 1986a. LFCM Vitrification Technology Quarterly Progress Report, April-June 1985. PNL-5470-3, Pacific Northwest Laboratory, Richland, Washington.

Burkholder, H. C., J. H. Jarrett, and J. E. Minor, compilers. 1986b. LFCM Vitrification Technology Quarterly Progress Report, July-September 1985. PNL-5470-4, Pacific Northwest Laboratory, Richland, Washington.

Goles, R. W., and G. J. Sevigny. 1983. Off-Gas Characteristics of Defense Waste Vitrification Using Liquid-Fed Joule Heated Ceramic Melters. PNL-4819, Pacific Northwest Laboratory, Richland, Washington.

Randall, C. T. 1982. Hazards Analysis of TNX Large Melter-Off-Gas System. DPST-81-914, Savannah River Laboratory, Aiken, South Carolina.

Savannah River Laboratory. 1983. Waste Management Technical Progress Report. DP-82-125-4, Aiken, South Carolina.

Scott, P. A., R. W. Goles, and R. D. Peters. 1985. Technology of Off-Gas Treatment for Liquid-Fed Ceramic Melters. PNL-5446, Pacific Northwest Laboratory, Richland, Washington.

CANISTER FILLING AND HANDLING SYSTEMS

D. H. Siemens and G. J. Sevigny

SUMMARY

The limited technical progress that took place this quarter will be reported in a future quarterly report.

INTRODUCTION

The objectives of this work are to develop and demonstrate systems for positioning canisters under the ceramic melter overflow; sealing the canisters to the melter overflow, and monitoring the glass level in the canister during filling. The objectives are also to develop and demonstrate systems for sealing and leak testing the filled canisters, and decontaminating the filled canisters. A turntable is used to position the canisters under the radioactive liquid-fed ceramic melter and the West Valley demonstration melter. A turntable is an enclosed tank that is sealed to the melter overflow with a carousel inside that supports and moves the canisters. Two methods (weight and gamma ray detection) are being developed to monitor the glass level in the canister during filling. Two turntable systems have been fabricated and tested; both systems are installed in their respective locations where operational testing is being conducted.

OFF-GAS SYSTEMS

R. W. Goles and C. M. Anderson

SUMMARY

Melter emissions and off-gas system performance studies have been conducted to evaluate the Hanford Waste Vitrification Project (HWVP) liquid-fed ceramic melter (LFCM) processing system. The overall system decontamination factors (DFs) established during testing were lower than expected primarily because of high formate-induced cesium volatility and inadequate performance of the high-efficiency scrubbers.

INTRODUCTION

Effluent emission and off-gas performance characterization studies are being conducted to establish processing criteria that will satisfy all pertinent licensing regulations governing future LFCM operations. The scope of these studies is quite broad and includes: establishing the nature and extent of melter feed component losses, characterizing the efficiencies of off-gas processing equipment, correlating melter exhaust composition with LFCM processing conditions, and identifying and/or monitoring potentially hazardous off-gas situations. The off-gas system performance is also included in the melter system technical progress.

TECHNICAL PROGRESS

An empirical evaluation of the reference HWVP LFCM processing system was completed during the last quarter. The basis of this evaluation was the 240-h pilot-scale ceramic melter test (PSCM-22) conducted during the last quarter of FY 1985. The melter off-gas system supporting this test was a scaled representation of the Savannah River Laboratory (SRL) Defense Waste Processing Facility (DWPF) reference design that included an off-gas film cooler, an

ejector venturi scrubber (EVS), a steam-atomized scrubber, (SAS), and a high-efficiency mist eliminator (HEME). The off-gas performance of the melter and each of these off-gas system components is discussed below.

Effluent sampling was conducted to characterize volatile and particulate releases from the PSCM and the scrubbing efficiencies of the off-gas equipment. Operational off-gas performance characteristics of the EVS and HEME were obtained throughout the experiment as were melter effluent emission characteristics. The performance of the SAS was evaluated during the last two days of testing. However, when not operating, the off-gas stream still passed through the SAS. The HEME was operated with and without a co-current water spray wash.

Feeds containing the formate anion can produce significant concentrations of H_2 and CO. Previous PNL melter tests involving the feeds formated at SRL have shown relative production rates of CO_2, H_2, and CO to be 1, 0.5, and 0.1, respectively (Goles and Sevigny 1983). The relative production rates of CO_2, H_2, and CO observed during this experiment were 1, 0.1, and less than 0.1, respectively. The presence of highly oxidizing NO_x gases in the melter exhaust may have been responsible for reducing the net off-gas yield of hydrogen produced.

Melter gas-phase losses to the off-gas system were significant only for B, C, N, S, and the halogens, which all readily form volatile acidic gases. This is consistent with previous testing (Goles and Sevigny 1983). The presence of sugar had no effect upon volatility in the melter. The halogen feed components had the ability to penetrate all off-gas processing equipment studied.

Since effluent gas-phase losses were limited to B, C, N, S, and the halogens, most melter off-gas system losses were associated with aerosol emission. Off-gas equipment performance can be measured in terms of decontamination factors (DFs): the ratio of the mass rate of a component exiting a device to the mass rate of that component entering the device. Therefore, the larger the DF, the more efficient the device. The average feed component DFs established for the melter, EVS, HEME, and the SAS throughout the experiment are summarized in Table 1.

The melter performance in terms of DF was quite consistent and reasonable. The very low Cs DF is associated with the presence of formate anion and is strikingly similar to previous PSCM data obtained during the processing of SRL-formated feeds (Goles and Sevigny 1983). Formated feeds appear to be exceptionally effective in promoting the Cs volatilization/condensation process in

TABLE 1. Average Elemental Decontamination Factors for the Melter and Off-Gas System

Element	Melter	EVS	HEME	SAS
Al	750.0	32.0	10.0	4.5
B	63.0	11.0	7.5	6.2
Ba	190.0	290.0	8.7	7.3
Ca	730.0	160.0	3.0	5.9
Ce	450.0	--	--	--
Cl	1.3	6.2	14.0	4.9
Cr	180.0	14.0	16.0	5.3
Cs	14.0	1.4	19.0	4.3
Cu	250.0	7.2	16.0	7.3
F	3.2	14.0	6.1	3.5
Fe	260.0	92.0	44.0	6.1
I	1.3	--	--	--
La	620.0	440.0	--	--
Li	500.0	2.6	19.0	5.0
Mg	630.0	94.0	1.0	1.2
Mn	300.0	220.0	36.0	5.5
Mo	57.0	1.6	19.0	4.8
Na	260.0	2.1	17.0	5.0
Nd	290.0	190.0	--	--
Ni	2100.0	3.7	64.0	6.1
Ru	42.0	1.4	32.0	4.8
S	1.8	4.3	18.0	2.3
Si	780.0	59.0	--	1.1
Sr	230.0	260.0	6.2	11.0
Ti	250.0	970.0	41.0	18.0
Zn	160.0	19.0	3.9	1.4
Zr	420.0	670.0	25.0	8.8
Total	180.0	5.0	5.6	1.7

the melter plenum. As a result, they have been responsible for the lowest recorded melter Cs DFs measured at PNL. It should be noted that the sugar component of the feed has no apparent influence on Cs or overall melter losses.

Like the halogens, sulfur exhibited a very low average melter DF of 1.8. The additional formic acid added with the frit addition (3 g/L of melter feed) must have been responsible for promoting high volatile loss rates of sulfur.

The total melter DF for Ru was determined only during one day when it was added directly to the melter feed tank. Its relatively low DF of 42 is indicative of an initial volatilization mechanism; however, its subsequent conversion to an aerosol was quite prompt because all detected Ru melter off-gas system emissions were confined to the aerosol sample fraction.

The performance of the EVS was quite predictable. This scrubber is a low-efficiency device that is designed to deal only with large-diameter aerosols. As a result, EVS elemental DFs should be direct measures of the mass mean diameters of the aerosols responsible for individual feed component losses. EVS performance during PSCM-22 is a reflection of the dominating influence of submicron aerosol losses on the overall melter source term. Conversely, gross feed entrainment was not an important melter loss mechanism during PSCM-22.

Because most aerosols penetrating the EVS are submicron, they all exhibited essentially the same HEME DFs. Effluents with volatilized components exhibited lower-than-average DFs. The variability associated with the HEME results in a reflection of analytical uncertainties at or near detection limits. The Cs DFs recorded during this experiment were a factor of about three higher than those observed during previous PSCM testing. These DFs, however, remain a factor of three below HEME design expectations. The reason for deficient performance may involve solution breaching of the filter element. Use of a water spray at the HEME inlet did not impact the HEME DFs. However, the mist carryover from the packed tower probably introduced as much moisture as did the 16-mL/min water spray when used. Only dry operation of the HEME has been successful in producing acceptable HEME performance (DF = 50) at PNL (Scott, Goles, and Peters 1985).

Most of the SAS elemental DFs observed during the experiment were lower than the values recorded for the HEME. Moreover, the DFs observed are not strongly element-dependent, which suggests that most aerosols penetrating the EVS are submicron. The single-stage Cs DFs observed during the experiment were an order of magnitude lower than design values of 50 for a dual-cascade SAS system (Randall 1982). If it is assumed that the combined DFs associated with cascaded SASs are the square of single-stage performance, the Cs DF for this test would have been ~20, which is significantly less than that recorded at SRL (1983).

CONCLUSIONS

The following conclusions are based on the work described in the preceding section:

- Results of off-gas characterization are consistent with previous experiments in which a melter feed pretreated with formic acid was processed.
- Off-gas equipment performance was consistent with past results.
- Efficiencies of the high-efficiency scrubber were below design expectations.

REFERENCES

Goles, R. W., and G. J. Sevigny. 1983. Off-Gas Characteristics of Defense Waste Vitrification Using Liquid-Fed Joule Heated Ceramic Melters. PNL-4819, Pacific Northwest Laboratory, Richland, Washington.

Randall, C. T. 1982. Hazards Analysis of TNX Large Melter-Off-Gas System. DPST-81-914, Savannah River Laboratory, Aiken, South Carolina.

Savannah River Laboratory. 1983. Waste Management Technical Progress Report. DP-82-125-4, Aiken, South Carolina.

Scott, P. A., R. W. Goles, and R. D. Peters. 1985. Technology of Off-Gas Treatment for Liquid-Fed Ceramic Melters. PNL-5446, Pacific Northwest Laboratory, Richland, Washington.

PROCESS/PRODUCT MODELING AND CONTROL

W. L. Kuhn, D. W. Faletti, L. J. Ethridge,
R. K. Farnsworth, and P. W. Reimus

SUMMARY

Progress is reported on simulation modeling of a vitrification system, further development of a heat transfer code, and predicting glass cracking from thermal history. A commercially available simulation language has been adapted for use in modeling a simple vitrification process. Plans for improving and upgrading the ability of the TEMPEST heat transfer code to analyze the filling and cooling of canisters are discussed. Correlations for predicting the extent of cracking in glass castings produced by liquid-fed ceramic melters (LFCMs) have been developed.

INTRODUCTION

The Nuclear Waste treatment program (NWTP) is a participant in the Waste Acceptance Process (WAP) convened by the DOE to assure that the waste forms produced by existing and future producers will be acceptable for disposal in licensed high-level waste repositories. Consequently the NWTP needs to define and implement a technical approach for addressing, evaluating, and meeting waste acceptance specifications.

A technical approach has been outlined that calls for development of product and process models as means for relating product quality to process measurements. Work on a product model has been supported to the extent necessary to understand the significance of results from process modeling, but the NWTP emphasizes development of process models because of their generality, as opposed to product models, which are more specific to particular waste form producers. The process model is divided into a mass balance model and a thermal model of the canister as it fills with glass and cools. The thermal model is mathematically sophisticated, but conceptually is simply a heat transfer

model for the canister/turntable system as glass is poured and cools. This section describes work done to develop and validate the process and product models.

TECHNICAL PROGRESS

Progress on simulation modeling, development of a heat transfer code, and prediction of glass cracking is discussed below.

PROCESS MODELING

Application of the SIMAN simulation language (Pegden 1985) has been demonstrated by modeling a simple vitrification system. The simplified system consisted of a makeup tank, a feed tank, a melter, and an off-gas system. Three process stream components were considered in the model: cesium, water, and a combination of all other constituents. Features of the model included a stochastic Cs concentration in the batches of waste charged to the makeup tank and a control system designed to apply corrective action when the Cs concentration in the glass is too high. The programming techniques developed in this initial application will be used to implement a more complex simulation as part of the NWTP waste form qualification effort.

TEMPEST VALIDATION

Although successfully applied in numerous other canister-filling and cooling situations, the TEMPEST heat transfer code could not be used with input parameters specific to the case of the 24-in.-diameter canister filled during a recent pilot-scale ceramic melter run (PSCM-21). The problem lay within the code, which has been partially corrected this quarter. Efforts are under way to fully correct the code.

TEMPEST CODE DEVELOPMENT

A plan for upgrading and improving the TEMPEST code has been developed. The major development areas for work contemplated in FY 1986 and FY 1987 include:

- improvement and updating of the continuous-pour adaptation of TEMPEST
- development of an exact radiation heat transfer solution for TEMPEST.

Improvement and updating of the continuous-pour adaptation of TEMPEST will involve the following:

- simplifying input requirements for the continuous-pour adaptation
- generalizing its application for all canister dimensions and process configurations
- including the ability to account for the viscid behavior of glass
- including the ability to handle all transients implicitly
- updating and inserting the adaptations into the latest referable version of TEMPEST.

Development of an exact radiation heat transfer solution will include:

- determining three or four approaches to use in attempting this development
- developing and inserting the preferred approach into the latest referable version of TEMPEST.

The ability of TEMPEST to compute radiation in an exact manner would significantly improve TEMPEST's ability to give thermal solutions for LFCMs.

CRACKING STUDIES

Methods to minimize crack surface area in waste glass castings and predict cracking as a function of thermal history have been developed. This work includes evaluation of both small-scale and full-sized glass canisters.

Fiberfrax®, a ceramic paper used for lining canisters, has been proposed as a means of reducing thermal stressing of glass during filling, cooldown, and decontamination of the canisters as well as for reducing glass/canister interactions. Eight lined canisters, four of which were heavily instrumented, were filled at PNL. All eight were sectioned radially and longitudinally to obtain

®Fiberfrax is a product of the Carborundum Company, Niagara Falls, New York.

qualitative information on the internal cracking. Two canisters were dismantled after the crack area was estimated using a crack intersect-fiduciary line technique. The relative area ratios for these canisters were small (3.5 and 7). Of particular significance was that no fines were observed and that there was no visible change in the Fiberfrax. Thermocouples placed within the glass did not increase localized cracking.

The amount of quantitative cracking information (or particle size data from which cracking area can be inferred) from canisters with known thermal histories was found to be quite limited. Data from four studies, in addition to the data obtained from the two canisters described above, provided data for 17 such canisters. These canisters ranged from 15 to 60 cm in diameter and from 80 to 290 cm in length. Cooling conditions ranged from very slow (phase cooling using an annealing oven) to very rapid (water immersion during and after filling). The canisters were made of either carbon steel or stainless steel. Four of the canisters were lined with Fiberfrax. Reported values of the relative surface areas (the ratio of the total surface area of the glass to the surface area of a glass monolith) ranged from 1 to 48.

A simple linear relationship between relative surface area (RA) and the radial temperature difference within the glass when its centerline temperature is 500°C (DELT) correlated with available data to within experimental uncertainties. The resulting correlation is:

$$RA = 1 + 0.085 \times DELT \text{ (for carbon steel canisters)}$$

$$RA = 1 + 0.19 \times DELT \text{ (for stainless steel canisters)}$$

The basis for this correlation is that, according to "quick freeze" models, stresses are locked into the glass if the glass is not isothermal as it passes through the transition temperature. Any subsequent change in temperature distribution following cooldown below the transition temperature (generally near 525°C) will result in stress buildups that can cause cracking. Therefore, the radial temperature difference when the surface temperature reached 500°C was chosen as a measure of the magnitude of these locked-in stresses.

When plotted according to the above correlation, i.e., for a given radial temperature difference, the surface area estimations made for the Fiberfrax-lined canisters did not show any reduced relative cracking area compared with the estimations made for unlined carbon steel canisters. This result is in conflict with the observations made during dismantling of the PNL canisters; these canisters appeared to have less than the normally expected cracking and had no evidence of fines. More extensive studies are recommended where direct comparison between lined and unlined canisters can be made.

The above correlation predicts relative surface area to within the accuracy of the existing data. However, more data are needed to validate this correlation.

CONCLUSIONS

The following conclusions are based on work conducted this quarter:

- The batch-wise operation of the vitrification process is amenable to simulation modeling, as has been demonstrated using the SIMAN code.
- The TEMPEST code needs specific improvements to more efficiently and accurately treat the analysis of glass canisters as they are filled and cooled. These improvements involve the continuous-pour adaptation of the code and development of an exact radiation heat transfer solution.
- A commercially available ceramic paper used as a canister liner reduced stresses and thus fracturing near the glass/canister interface in the castings. Use of such paper is proposed as a relatively simple step to improve the quality of castings.
- The extent of fracturing in solid cylindrical glass castings has been found to correlate linearly with the radial temperature difference.

REFERENCE

Pegden, C. D. 1985. Introduction to SIMAN. Systems Modeling Corporation, State College, Pennsylvania.

SUPPORTING STUDIES

K. J. Schneider, Compiler
L. R. Bunnell, G. D. Maupin, and W. L. Partain

SUMMARY

A report was written that provides the rationale supporting the design of the high-level waste vitrification system for the West Valley Demonstration Project (WVDP). Possible alternatives to the chosen design and references supporting the technology are discussed. This report in conjunction with the project drawings provides the technical bases for designing a vitrification system.

As part of the effort to discover and evaluate viable second-generation waste forms, glasses with processing temperatures higher than 1100 to 1200°C are being examined. Low alkali, high alumina-boron glasses processed at 1400°C and containing 25 wt% simulated reprocessed commercial nuclear waste have been fabricated and evaluated for chemical durability. These glasses exhibit matrix dissolution rates an order of magnitude lower than current reference glass compositions over a wide range of conditions analogous to repository flow rates and time.

All of the data collected to compare the leaching performance of Synroc-C with PNL 76-68 glass were combined and analyzed. In most cases, release rates appear to be reaching final values, and Synroc-C is seen as being superior to the 76-68 glass by about an order of magnitude.

INTRODUCTION

The objective of these supporting studies is to carry out technical analyses that provide input and guidance for development of vitrification technology. Studies are being performed that support various aspects of nuclear waste vitrification technology development. These studies include generic

assessments of vitrified waste performance during subsequent waste management operations, development of requirements/criteria for vitrified waste, assessment of alternative waste forms, and documentation of vitrification technology and plans for specific applications.

TECHNICAL PROGRESS

Progress on three supporting studies is discussed in this quarterly report: West Valley vitrification system equipment design, high-temperature waste glass evaluation, and Synroc-C evaluations.

WEST VALLEY VITRIFICATION SYSTEM EQUIPMENT DESIGN

Pacific Northwest Laboratory (PNL) and West Valley Nuclear Services, Inc., designed the principal vitrification system components for the West Valley vitrification project (Siemens et al. 1986). A document was prepared as one means of transferring this technology to other applications. The report describes the design features of the principal vitrification equipment as shown in Figure 1. Each of these equipment pieces is discussed within the context of design criteria, performance objectives, detailed description, design analysis, features for remote operation, instrumentation, potential operating upsets, and alternative concepts for the design. Highlights of the information are given below.

Concentrator/Feed Makeup Tank

The concentrator/feed makeup tank (Figure 2) serves as a waste receiver, reactor, evaporator, feed makeup tank, and feed tank. The tank receives cesium-loaded zeolite slurry, reprocessing sludges, and thorium waste from existing tanks at West Valley. These waste solutions are transferred in predetermined amounts to provide individual batches with satisfactory melter feed composition. After receipt of the waste, nitric acid is added to convert the waste to its nitrate form. The blended nitrated waste is then concentrated to remove excess water. Finally, glass-forming chemicals are added to the solution.

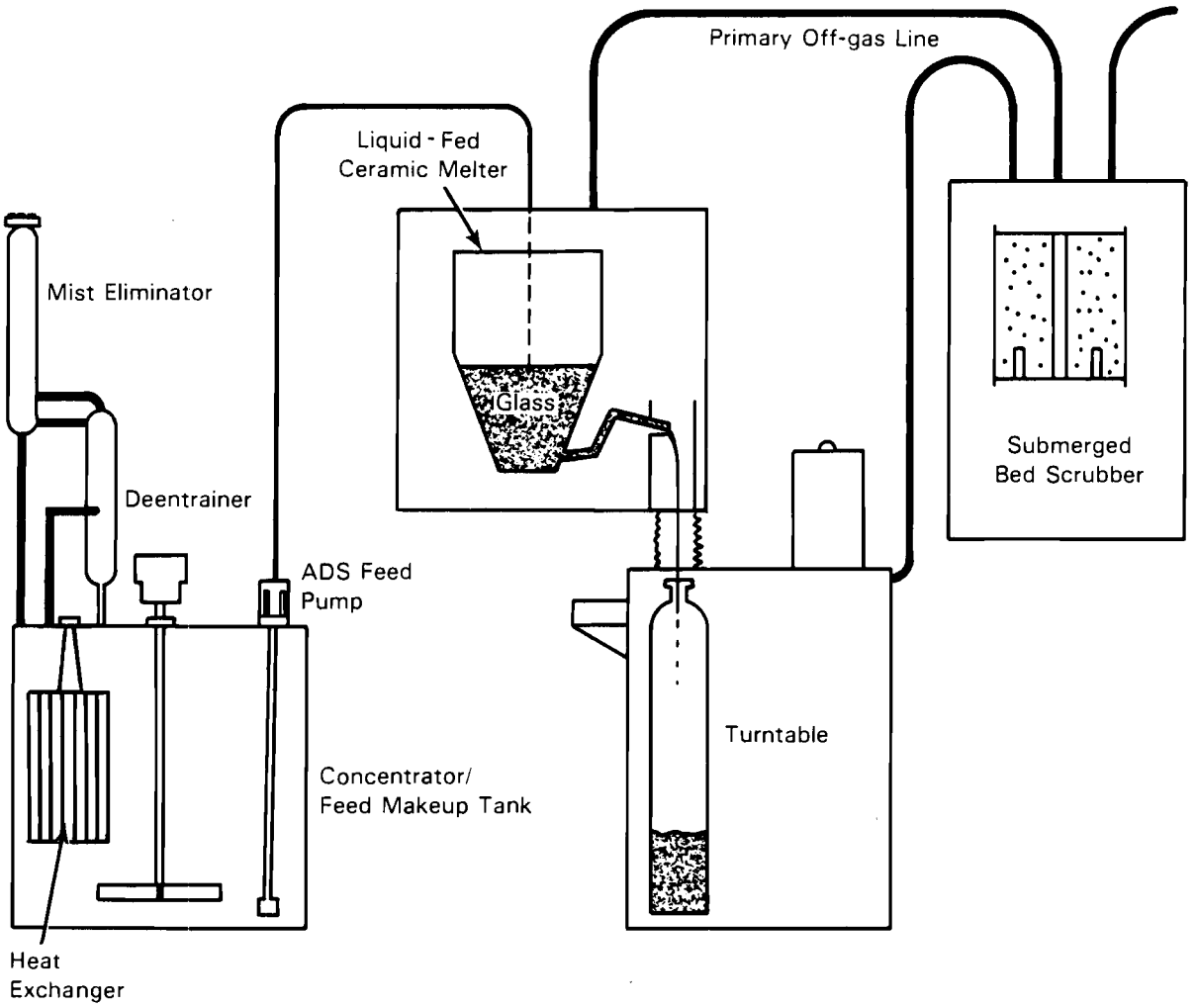

FIGURE 1. Schematic of West Valley Vitrification Equipment

The tank has a working volume of about 500 gal. Its outside diameter and height are determined by the dimensions of the installation site. The best liquid height-to-diameter ratio for solids suspension was calculated as approximately 0.8. The 8-ft liquid height in a 10-ft diameter tank is within the suction lift capability of a steam transfer jet.

Calculations indicated that solids suspension and homogenization can be achieved throughout 90% of the tank volume by a 15-hp agitator with a 35-in. impeller. Four 10-in.-wide baffles that stand 1-5/8 in. off the wall eliminate vortexing of waste solution during agitation. Baffles are sized at 1/12 of the

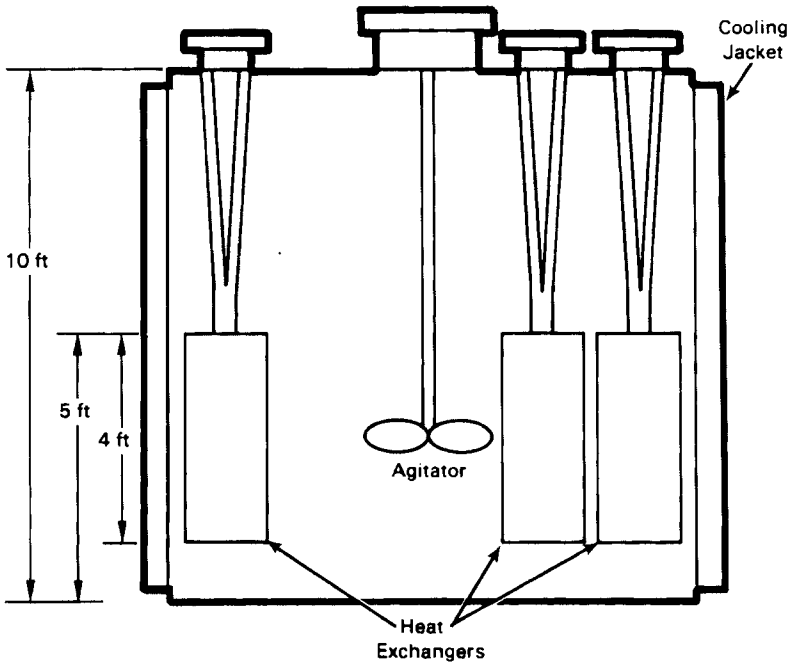

FIGURE 2. Concentrator Feed Makeup Tank

tank diameter and offset from the wall 1/72 of the tank diameter from calculations of ratios that are typical for solutions with a viscosity close to water.

The aqueous makeup tanks in the facility supply the measured amounts of process nitric acid and can also supply decontamination solutions. Samples can be taken through a sampling nozzle.

The nitrogen oxides produced in the nitration reaction are vented into the tank vent system, which consists of a deentrainer, a mist eliminator, and a condenser. The rate of nitrogen oxide evolution will be controlled by limiting the addition of nitric acid to a volume that can be handled by the ventilation system without pressurizing the tank.

Concentration of the waste solution is provided by three reboilers, each consisting of 53 heat exchanger tubes (1-1/2-in. diameter and 48-in. long). Steam is on the outside or shell side of the tubes, and the waste solution circulates by natural convection up through the tubes where evaporation takes place. The reboilers are designed for crane replacement by suspending each reboiler from a flange on the top of the tank.

Following the nitrification and evaporation phase, the concentrated waste slurry must be cooled. The design specification calls for cooling the feed slurry to 50°C within 8 h, which takes into account the substantial cooling effected by adding the glass formers to the concentrated waste slurry. A cooling jacket was selected for the cooling process instead of coils primarily because it has a lower pressure drop for the cooling water. The cooled feed slurry is stored in the tank where it is agitated and kept at the proper temperature while the pump located on the tank lid meters it to the melter.

Concentrator Deentrainer and Mist Eliminator

The deentrainer and mist eliminator are the first treatment stages in the vessel vent system for the off gases from the concentrator/feed makeup tank. The deentrainer and mist eliminator remove entrained liquid droplets of 5 μm or larger from the vapor driven off during the evaporation process.

The deentrainer and mist eliminator are constructed as a single unit for the purpose of remote repair as shown in Figure 3. Vapor from the concentrator/feed makeup tank enters the equipment, and liquid droplets and condensate that are removed in this equipment are drained back to the tank. The vapor passing through this equipment goes into a condenser and into the facility off-gas system.

The deentrainer and mist eliminator are designed based on relationships given by Ludwig (1980). The deentrainer and mist eliminator are sized to reduce the vapor velocity to 10 ft/s so that the larger liquid particles can settle out. The mist eliminator incorporates two 6-in. wire mesh pads spaced to provide 18 in. of disengaging space ahead of the inlet face of either mesh pad and 12 in. of disengaging space before the vapor leaves the mist eliminator.

The design is based on a vapor production rate during evaporation of 305 kg/h. It should be relatively effective for vapor velocities of 20% to 120% of this value. If velocities are too low, the particles do not impinge on the mesh and may be carried through; if velocities are too high, the vapor may reentrain liquid from the mesh pads.

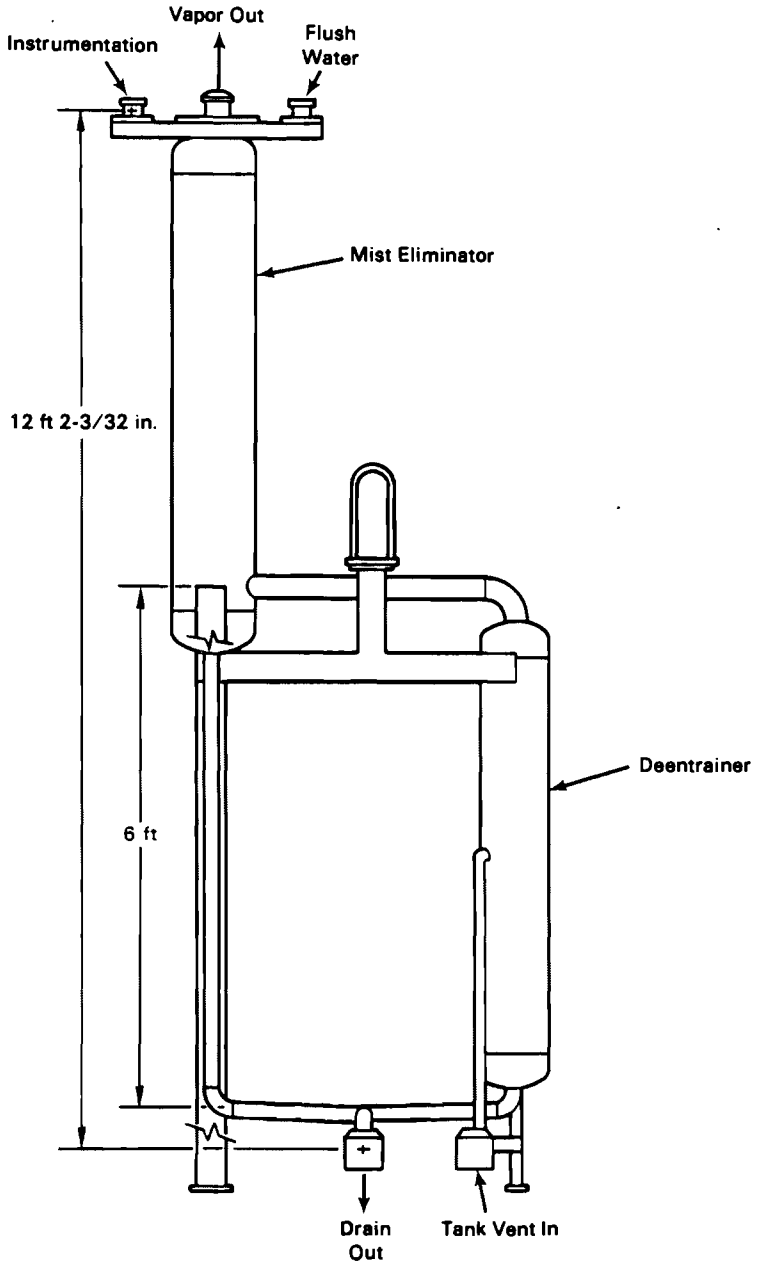

FIGURE 3. Concentrator Deentrainer and Mist Eliminator

Submerged Bed Scrubber

The submerged bed scrubber (SBS) provides the first stage scrubbing of melter exhaust gas. It also serves to cool and condense the melter off gas, temporarily storing the condensate in its outer annulus. A schematic of the SBS is shown in Figure 4.

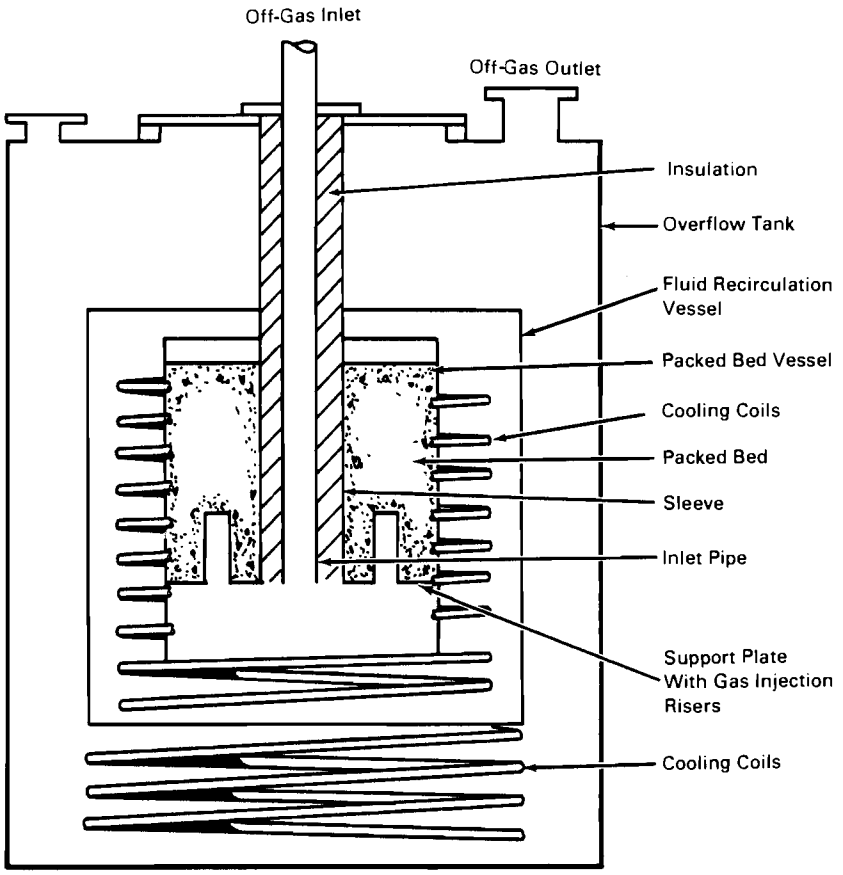

FIGURE 4. Schematic of the Submerged Bed Scrubber As Designed by PNL for West Valley Nuclear Services

The SBS is a passive device and requires no external pump or tank for its scrubbing action. Liquid circulation in the packed bed is induced by the buoyant effect of the rising gas. This liquid motion facilitates the gas cooling and scrubbing functions of the SBS and also keeps the packing of the bed clean, thus preventing plugging.

The packed bed cross-sectional area is sized to achieve a superficial gas velocity of approximately 75 ft/min through the bed. Gas velocities from 30 to 110 ft/min provide good scrubbing action in the packed bed (Hilliard et al. 1981). The bed cross-sectional area is 6.9 ft^2 and the height is 38 in. The bed is formed from 3/8-in. ceramic spheres. The bed injection plate utilizes two gas injection risers that are 10-in. high and 4-in. wide with 1/4-in. slot openings. The free area of these risers is 100% of the superficial column area.

The packed bed and its recirculation vessel are contained within an overflow tank. The overflow tank provides lag storage for condensate collected by the packed bed, which overflows from the recirculation vessel. The overflow tank is 11 ft 4 in. high and 8 ft in diameter. The capacity is 1450 gal (5481 L), which is sufficient volume to hold all of the melter steam emissions (115 kg/h) for about 48 h. Fluid is transferred from the overflow tank batchwise using a jet eductor pump.

Three independent oversized cooling coils are incorporated into the SBS; two surround the packed bed and one lies below the bed in the overflow tank.

Air Displacement Slurry Pump

The air displacement slurry pump (ADS) is a feed metering system that transfers a waste and glass-former slurry from the concentrator/feed makeup to the melter at rates of 50 to 200 L/h. The waste and glass-former slurry can contain more than 50 vol% solids, which are erosive and tend to settle into areas of low slurry velocity, thus clogging orifices and valves. Caustic feeds tend to produce salt deposits at air/slurry interfaces, cementing the particles together and plugging those interfaces. In addition to these chemical and particulate qualities of the slurry, radioactive waste mixed with glass formers will deliver high alpha, gamma, and beta dose rates to the pump parts. Elastomers that are typically used in pump design cannot be used because they are damaged by radiation in a short time period.

The feed must be delivered to the melter at variable rates but at a low pressure so that it will not be injected significantly below the molten glass surface. At PNL, remote operation involves a direct delivery melter feed system that does not depend on a flow control valve or a flow measuring device in the slurry stream or require priming of the pump. Only top entry is permitted in remote tank design; therefore, the pump must lift slurry from the feed tank through a port in the lid of the tank. Frequent replacement or adjustments to compensate for erosion or plugging are undesirable in a remote operation where all servicing is performed with a bridge crane or master/slave manipulators.

An extensive review of commercially available pumps, present industrial practices, and applicable pump literature was made to identify the most likely

candidates. Two candidate systems, the ADS pump and the two-stage air lift pump, were chosen for additional development work and extensive testing. Long-term continuous testing of these pumps was conducted during FY 1984. Both concepts successfully operated for more than 720 h.

The ADS pump was chosen for further development and for use in the WVDP because it showed better metering capabilities than the two-stage air lift pump when the feed slurry contained particles, such as the zeolite that is to be incorporated into the WVDP feedstream. The ADS pump was proven in over 4000 h of nonradioactive test operation in the Hanford Waste Vitrification Program development work (Blair and Peterson 1984).

The ADS pump is shown in Figure 5. The pump chamber is submerged in the feed makeup tank 0.5 in. from the bottom. The chamber has a volume of approximately 2 L, which enables flow rates of 50 to 200 L/h and minimizes any slurry holdup in the chamber.

A controller must sequence and control the four steps of the operating cycle. During the first step of the cycle, the two-way valve is driven upward, and slurry flows into the pump chamber and at the same time closes off the feed line going to the melter. The second step is the time period allowed for slurry to flow into the pump chamber. Since slurry flows into the chamber as a function of the tank head, the time for Step 2 must be adjusted as the tank head decreases. In order for the controller to automatically make this adjustment, input into the controller from a tank level sensing device is required. Otherwise, the adjustment can be made manually by an operator. The air, which is in the chamber prior to filling, is vented through the air/vent valve back into the feed makeup tank. In the third step, the two-way valve is driven downward, closing the port into the tank and opening the feed line to the melter. The fourth step of the cycle is the actual discharge of the slurry. Air pressurized from 0 to 20 psig forces the slurry out of the feed line and into the melter. These four steps create a pulsating flow pattern during the pump operation.

The pneumatically activated two-way valve is a special feature of the pump design. The two-way metal valve seats against two machined metal surfaces. The chamfered surfaces provide adequate sealing that prevents large volumes of

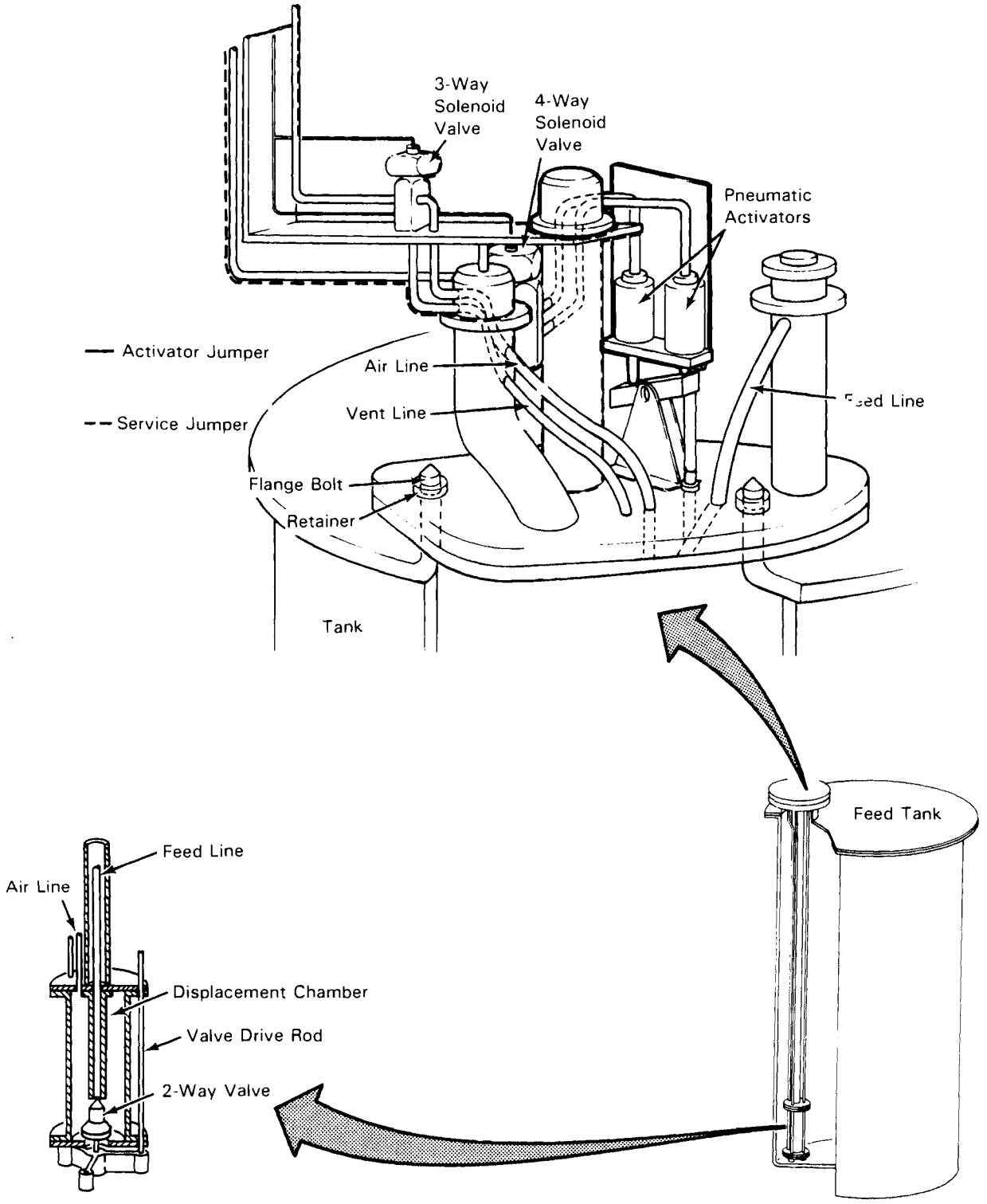

FIGURE 5. Air Displacement Slurry Pump for the WVDP

motive air leakage into the tank or feed line. Large quantities of air leaking into the tank reduce pump efficiency, and air leakage into the feed line increases the melter off-gas system requirements and tends to cool the melter plenum.

The actuator assembly for the two-way valve was changed significantly from previous designs to allow for remote replacement of the activator. Two pneumatic cylinders actuate the valve by means of a drive rod and drive mechanism. A single drive rod was selected to minimize the number of seals required on the tank flange. Motive air enters the pump chamber through 0.5-in. Schedule 40 pipe and slurry exits through the 0.38-in. Schedule 40 pipe. The tolerances, assembly and component design, and selection of hardened stainless steels improved the valve alignment and sealing. Guide bushings are used on the two-way valve and on the drive rod to assure the alignment of the valve and seating surface. The inside surfaces of the chamber have been designed to minimize areas for solids to deposit and collect. Pump components are machined to prevent solids from collecting in irregularities and forming potential plugs. To prevent foreign material from becoming wedged in the feed line, a screen with mesh openings slightly smaller than the inside diameter of the feed line was installed over the entrance port.

The pump is fabricated of 304L stainless steel except for the two-way valve, the valve seats, and guide bushings, which are made from an age-hardened stainless steel. The pump is mounted to a flange on the tank.

Two double-acting pneumatic cylinders provide the vertical push-pull motion that operates the two-way valve, which is located on the inlet of the pump slurry chamber. A solenoid valve regulates the air to the pump chamber while another solenoid valve controls the air to the pneumatic cylinders.

Turntable

The turntable is a large cylindrical enclosure located below the melter. Inside the enclosure a carousel holds four canisters and rotates the canisters into position below the melter discharge for filling. The turntable concept provides a method for moving canisters for filling, controls the spread of contamination to the process cell, controls air inleakage to the melter off-gas

system, and incorporates canister weighing and glass level detection instrumentation. The turntable must accommodate canisters that are 0.61 m in diameter and 3.05 m tall.

A side view of the turntable assembly is shown in Figure 6. The turntable is supported by an external framework and moved into position underneath the melter on a rail system. The turntable shell is connected to the melter discharge port by an expandable metal bellows. Canisters are loaded in through the seal port and rotated into position by the carousel inside the shell. There are two fill stations corresponding to the two melter discharge openings. However, only one fill position is ever in use at a time; the other is a backup.

The turntable shell surrounds the carousel and, in conjunction with the supporting frame, provides the structural support for the system. The shell is connected via a vent line to the melter and operates at the same negative pressure. This design makes it unnecessary to couple each canister individually to the melter for off-gas vacuum control. The shell concept also reduces the spread of contamination to the cell.

The canisters give off significant heat due to the sensible heat of the molten glass plus any radioactive decay heat contained in the glass. The turntable shell has water jackets to remove heat from the glass. The lid of the turntable is removable to allow retrieval of the canisters if the turntable drive system irrepairably fails.

Four permanent cylinders are attached to the carousel on a central vertical axle. Approximately one-half of the weight of the cylinders is supported from the vertical axle, while the remainder is supported by wheels riding on a rail attached to the turntable shell. Inside each cylinder is a removable thimble in which the waste canisters are placed. The radial positioning of the canisters is monitored by a linear variable differential transmitter that detects different height cams mounted on the carousel.

The turntable is maintained at essentially the same negative pressure as the melter by a 6-in.-dia connecting line. A controlled air flow is introduced

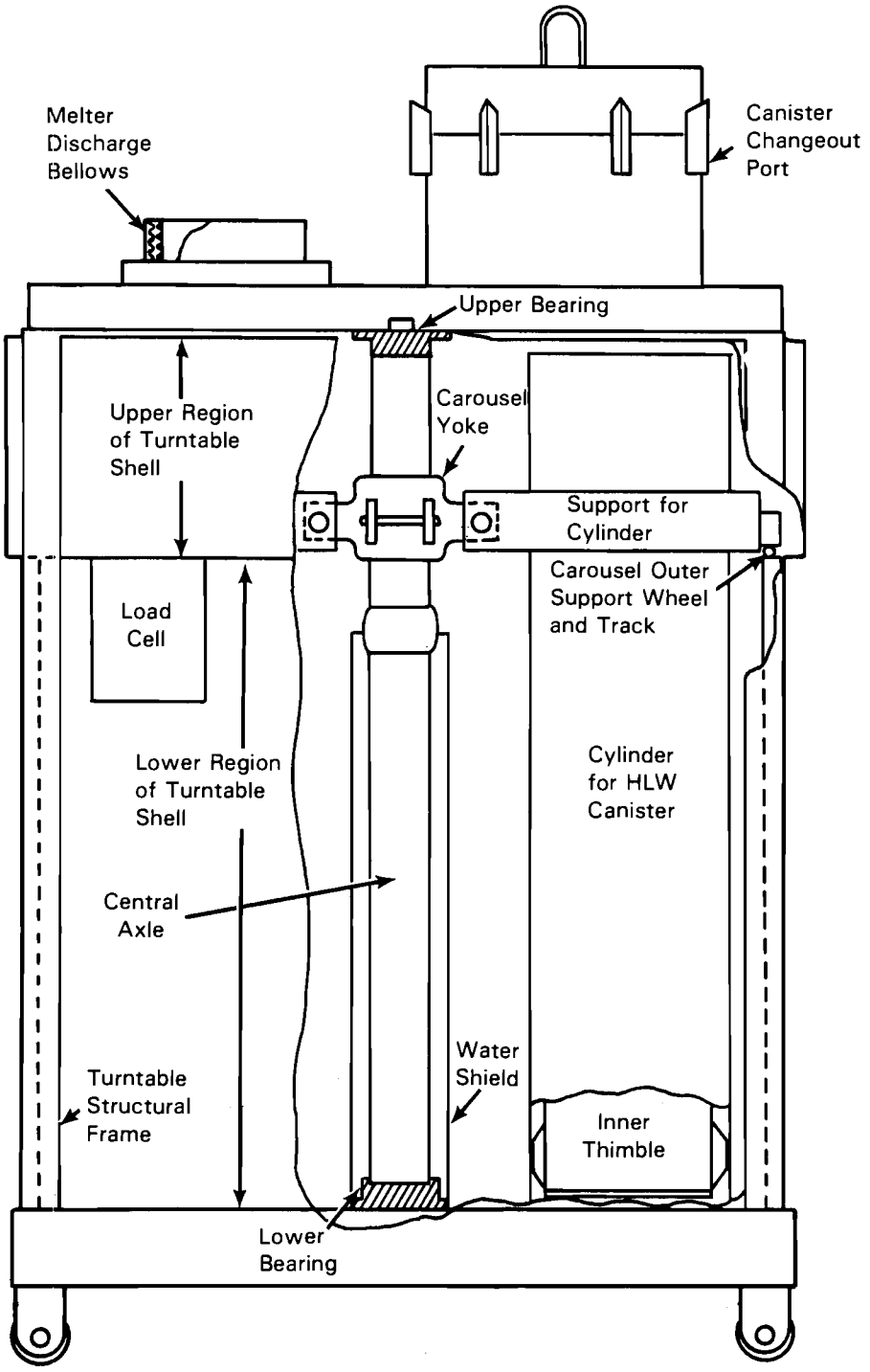

FIGURE 6. Cutaway View of the Turntable Assembly

into the turntable to reduce the buildup of contamination and this air then flows into the melter and out the primary off-gas vent line.

An alternative flow path for off gas is provided through the turntable to the SBS, with approximately 6-in. water gage higher static pressure than the primary path under normal operation. Therefore, if the pressure drop through the primary off-gas pipe increases beyond this static head, the melter off gas will begin to vent to the SBS through the turntable.

The canister changeout port on the turntable has a water seal. An over-pressure of ~15-in. water gage in the turntable will have to occur before the turntable is vented to the cell atmosphere.

During continuous operation, a canister must be removed and a new one inserted into the turntable about every two days. The changeout port has been designed to minimize air inleakage during the canister changeout.

The turntable ports are connected to the melter by a double-walled bellows that is inflated to seal against the melter. In accordance with the design criteria, this bellows can be removed and the turntable removed from its operating position while the melter remains at operating temperature.

There are two means of determining the glass level within the turntable. The canisters are weighed when in the fill position, and a vertical array of collimated gamma detectors positioned just outside the cell wall determines the approximate level of the radioactive glass.

Melter

The principal features of the melter are shown in Figure 7. The glass-melting furnace is a ceramic-lined cavity inside a metal containment vessel. Energy for melting the waste slurries is generated within the molten glass pool by passing an alternating current between three electrodes. The melter has a glass surface area of approximately 2.15 m^2 and a maximum slurry processing rate between 130 to 175 L/h (60 to 80 L/h-m^2). The design glass rate for the melter is 45 kg/h. This glass rate is achieved at a slurry feed concentration of approximately 350 g-oxide/L and a processing rate of 130 L/h.

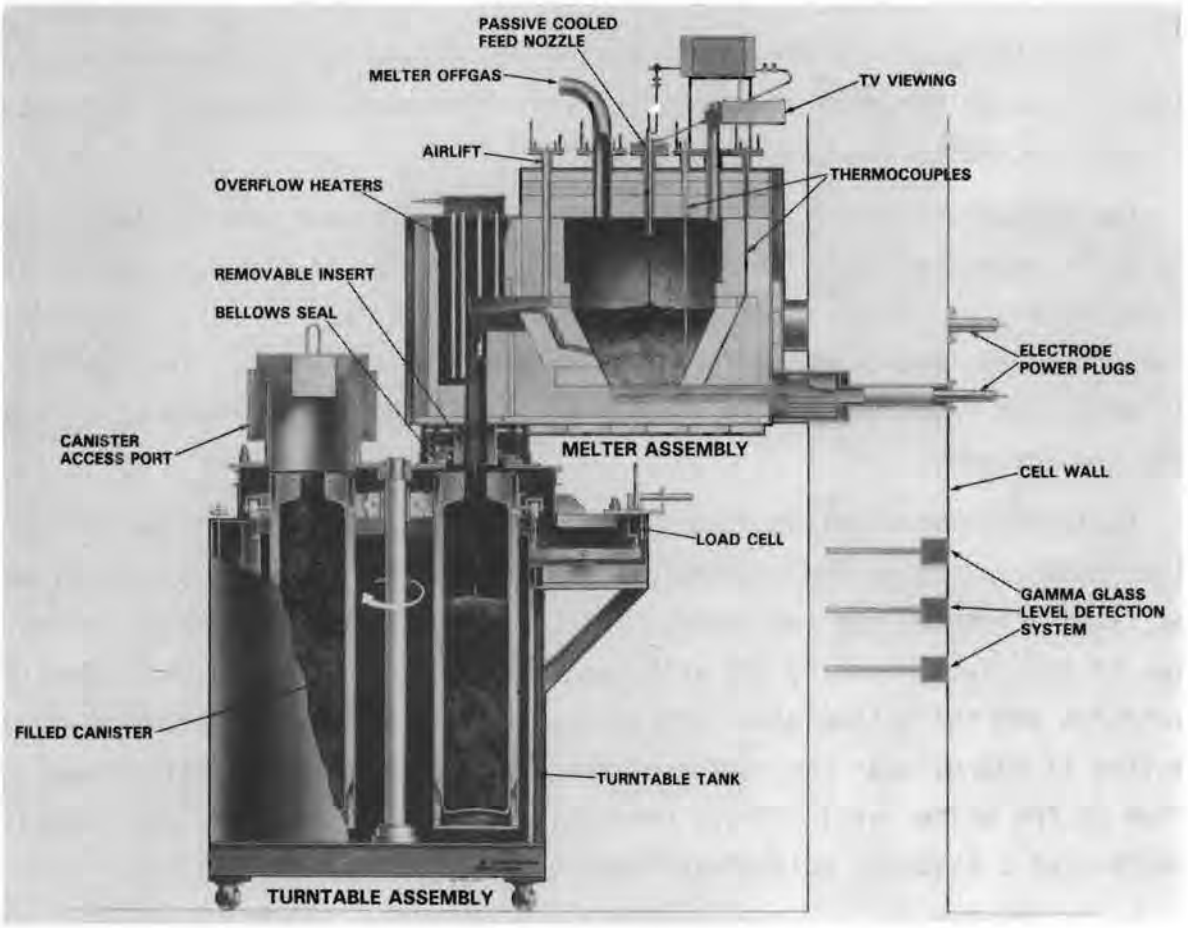

FIGURE 7. West Valley Vitrification System

The floor and the bottom 75% of the walls are water cooled to reduce the heat load on the cell ventilation system and to minimize the overall weight and size of the melter through the use of less refractory insulation in the walls. The melter weighs approximately 55 tons, and the external dimensions are 10.75-ft long x 10.6-ft wide x 9.67-ft tall. The melter must be rolled into the vitrification cell and positioned above the turntable on a suspended rail system because its weight exceeds the capacity of the cell crane.

The glass-melting cavity dimensions at the normal glass level are 68-in. long, 49-in. wide, and 10- to 26-in. deep. The inverted pyramid-like melter cavity shape was selected to improve the structural stability of the melter's

refractory lining and to reduce the molten glass inventory. The maximum glass volume in the melter when new is 860 L, which increases somewhat as refractory corrosion increases the cavity volume.

The melter utilizes three electrodes. Two electrodes are located on opposite walls near the glass surface, and the third forms the lowest portion of the melter floor. These electrodes are air cooled to permit bulk glass temperatures up to 1300°C. The electrodes extend from the melter, through the cell wall, and into the service gallery to permit contact maintenance of the power connections.

Analytical and modeling studies indicate that a three-electrode design allows good control of the temperature profiles in the glass. Electrical current flowing between the two sidewall electrodes will deposit energy in the top layer of the glass close to the cold cap, while current between the sidewall electrodes and the bottom electrode can be controlled to deposit the desired fraction of energy near the bottom of the melter. The heat deposited near the bottom of the melter will enhance convective mixing of the glass and prevent formation of a viscous, cold glass layer on the bottom of the melter.

The connection bus bars for the three electrodes extend out through the sidewall of the melter and through special penetrations in the cell shielding wall. A cutaway view of a complete electrode assembly is shown in Figure 8. The electrical connections are made outside the cell where they will not be exposed to the corrosive cell atmosphere and where they can be maintained more easily. The sidewall electrode penetration as opposed to penetration upward through the melter lid also provides more space on the lid of the melter for other required melter penetrations. The sidewall penetrations do require more extensive cooling to prevent glass migration along the electrode to the melter containment.

Two overflow glass discharges are provided. Only one discharge will be used at a time. The second discharge is provided as a backup because some postulated failure modes of the discharge may be difficult, or impossible, to repair remotely.

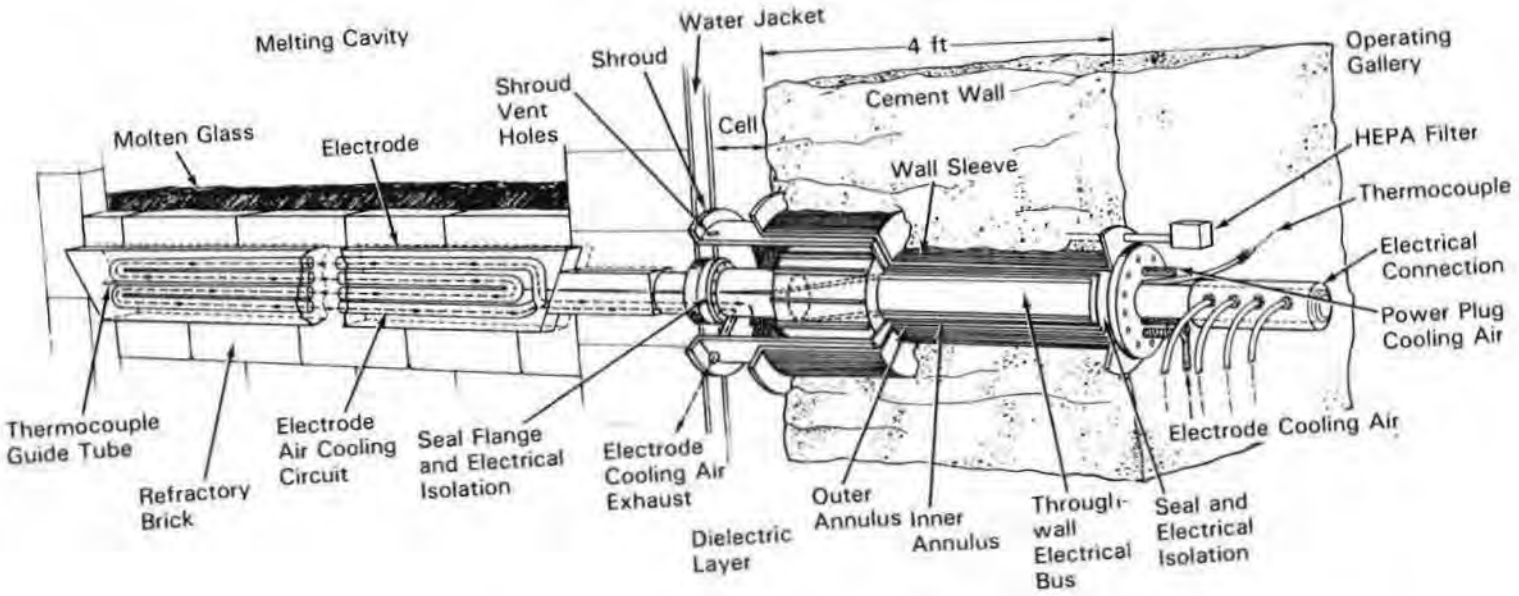

FIGURE 8. Perspective View of a Melter Electrode

The melting cavity has a 36-in. plenum area above the glass level, which reduces the particulate loading of the off-gas stream, reduces the probability that the off-gas line will become blocked by glass foam or dried feed splatter, increases the remote video viewing angle, and allows room for various melter restart techniques.

The outer melter dimensions are determined by adding the necessary layers of refractories, insulation, metal shells, cooling jackets, and flanges around the melting cavity. The glass discharge section on one side of the melter increases the overall dimensions of the melter.

The melter design is principally an evolution of the development work that has been carried out at PNL over the past decade in the adaptation of the technology for industrial electric glass melting to the vitrification of nuclear waste.

HIGH-TEMPERATURE NUCLEAR WASTE GLASS EVALUATION

Studies are in progress to examine the potential of higher temperature commercial waste glasses (i.e., glasses formed and melted at higher temperatures) with respect to chemical durability (i.e., leaching by water). Higher temperature glasses generally exhibit superior durability relative to low-temperature glasses but are more difficult and costly to process. Recent studies indicate the liquid-fed ceramic melter (LFCM)--currently operated at 1100 to 1200°C--could be modified to operate at 1400 to 1500°C. The increased cost of building and operating a high-temperature LFCM may be justified by a significant, perhaps an order of magnitude, improvement in the resulting chemical durability of the waste form.

Initial development and testing of glass compositions with viscosities of about 100 poise at 1400°C and incorporating 25 wt% simulated PW-4b waste involved modification (increased silica content and substitution of PW-4b waste) of current LFCM glass compositions. These "analog" glasses, however, were only about twice as durable as current reference LFCM glasses. The analog approach was subsequently abandoned; developmental efforts shifted towards less conventional glass compositions that were investigated in the form of a substitution study and a statistically designed empirical mixture study (EMS).

Initially, the glass form substitution and empirical studies yielded a factor of about five improvement in chemical durability. Recent efforts have concentrated on expanding the experimental field and increasing the resolution and range of chemical durability data for the EMS.

The original hexagonal experimental field is represented in the overall ternary field in Figure 9. The EMS was designed such that the molar ratios of flux components: alkali, boron, and alumina, varied. The waste-loading (25 wt%) and viscosity (100 poise at 1400°C) of the compositions, however, were held constant by allowing the flux-to-silica ratio to vary. The chemical durabilities of seven compositions representing the hexagonal field were measured using a MCC-3, 7-day test. The boron and silica release data were empirically modelled as a function of flux composition. The models predicted the most durable glass to be a low alkali, high boron-alumina composition located on the extreme edge of the original experimental field. Subsequent testing of the predicted "optimum" glass seemed to verify the models and implied that even more durable glass compositions might exist outside of the original field.

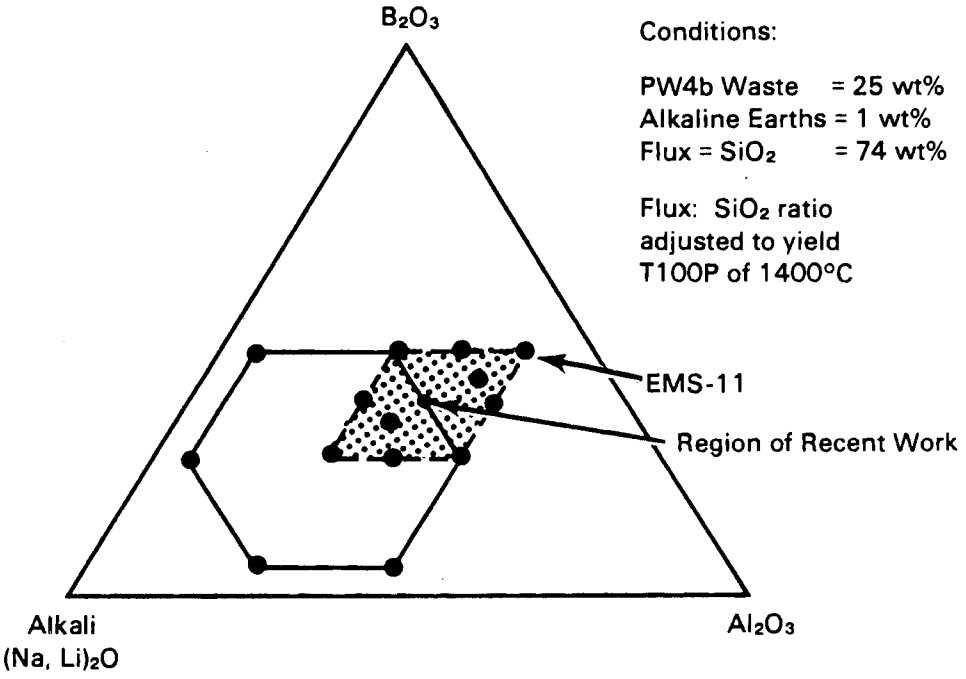

FIGURE 9. Ternary Diagram of the Compositions Evaluated in the Empirical Mixture Study. The shaded parallelogram represents the region of recent work; compositions are represented by dots.

The experimental field has been enlarged, and the number of samples has been increased as indicated by the shaded region in Figure 9. Although testing is still in progress and modeling is yet to be done, it is apparent that at least one composition, EMS-11[a] (see Table 1 for composition), has exceeded a factor of 10 improvement in chemical durability relative to SRL-165 glass[b] at 90°C in deionized water. The bar graphs in Figure 10 compare the elemental releases of PNL 76-68, SRL-165, and EMS-11 glasses in 7- and 28-day MCC-3 testing. For boron release rate, which is considered to be the most representative indicator of matrix dissolution rate, EMS-11 exhibited an average matrix dissolution rate 45 times lower than PNL 76-68 and 10 to 12 times lower than SRL-165. Considering the other elements, the strontium release rate at 7 days appears somewhat high for EMS-11 but is a factor of two better than SRL-165 at 28 days. There is incongruent leaching of lithium from EMS-11 that is not understood, but it does not appear to be a problem.

TABLE 1. Composition of EMS-11 Glass as Determined by Inductively Coupled Plasma Analysis

Oxide	wt%	mole %
Al_2O_3	20.59	16.34
B_2O_3	13.42	15.60
CaO	0.59	0.84
Li_2O	0.60	1.61
MgO	0.52	1.05
Na_2O	1.21	1.58
SiO_2	38.86	52.34
PW-4b	24.21	10.62
	100.00	100.00

(a) Attempts to produce 1400°C glasses having flux compositions just to the right of EMS-11 (Figure 9) have been unsuccessful because the viscosity is too high.

(b) This glass is a nonradioactive version of SRL-165 that was prepared and tested at PNL and is considered to be comparable to the current West Valley and Hanford "working glasses."

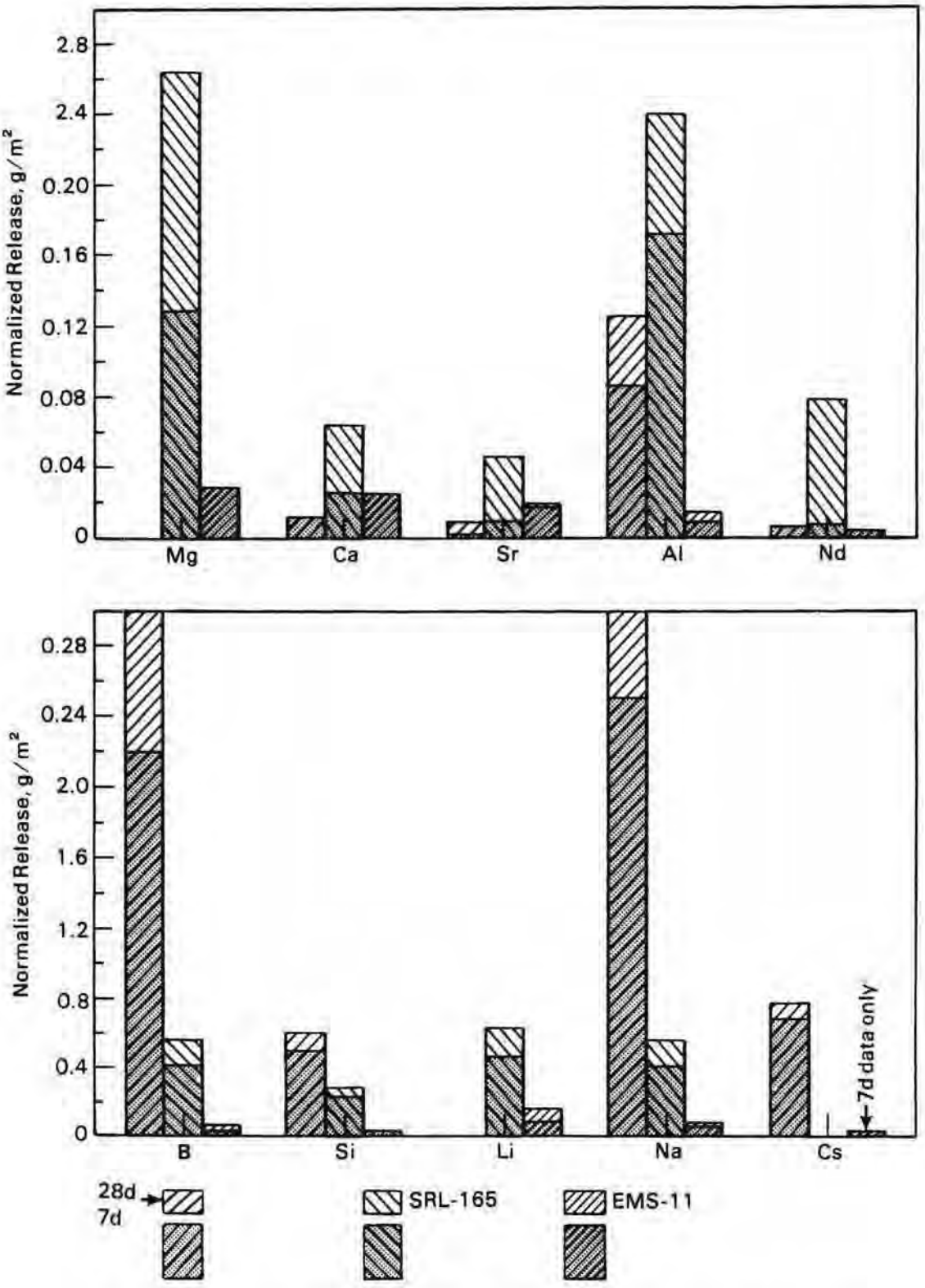

FIGURE 10. Comparison of Element Releases Among Glasses

In addition to increasing the number of samples (which should allow greater resolution and accuracy in predicting optimum compositions) other refinements have been made to the shaded portion of the EMS (Figure 9). Two newly developed ways of looking at leaching data are being used to evaluate the samples at conditions analogous to very high flow rate, short-term exposure such as in some shipping accidents and to low flow rate, very long-term exposure conditions encountered in a repository. Figure 11 illustrates how these data can be used to compare the relative chemical durability behavior of glasses in a way that is relevant to long-term repository performance.

In Figure 11, normalized boron concentration is presented as a function of surface area of the leach sample divided by the volume of the leachate (SA/V) multiplied by the leaching time [(SA/V) x time]. A high [(SA/V) x time] value is analogous to typical flow rates and time in a repository. Low values are

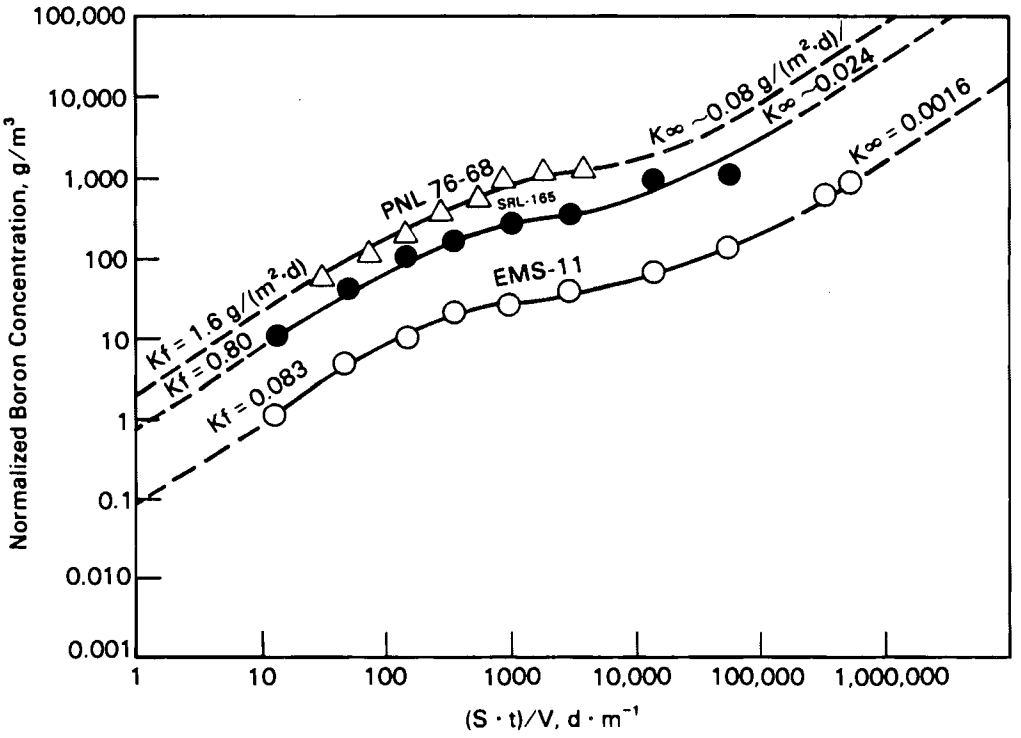

FIGURE 11. Comparison of Relative Chemical Durability Behavior Relevant to Long-Term Repository Performance

analogous to short-term events such as shipping accidents. For a given SA/V ratio, the change in normalized boron concentration with time is equal to the glass dissolution rate.

Figure 11 is presented as a log/log plot because of the large range of numbers being considered. For the purpose of illustration, assume that the flow rate and surface area of exposed glass in a repository is equal to an SA/V value of 1 m^{-1}. The X-axis can now be regarded as simply log[time]. On a log/log plot, a slope of one (or unit-slope) indicates a function having a constant rate of change, and the Y-intercept at X = 1 (time = 1 day) is that actual rate. Looking at Figure 11, the dotted lines at short times (1 to 100 days based on the assumed SA/V ratio of 1) represent "forward rates of reaction" for PNL 76-68, SRL-165, and EMS-11 glasses. The approximate values for these forward rates based on the intercepts are indicated as K_f; at short exposure times (or very high flow rates) EMS-11 appears to be about 10 times more durable than SRL-165 and 20 times more durable than PNL 76-68. The dotted lines at very long times (at the assumed SA/V ratio equivalent to times greater than 10^6 days or 27,000 years) represent theoretical "final rates of reaction" (represented as K_∞) that are believed to exist based on geochemical models and some experimental data.

Clearly, further testing is needed to confirm the validity of such models; however, the data represented in Figure 11 imply that EMS-11 is more than a factor of 13 better than SRL-165 at longer leaching times, based on element release indicative of matrix dissolution. Modeling of the revised EMS glass has been delayed to incorporate the type of data represented in Figure 11. This modeling may reveal even better-performing glasses in the composition field, or it may confirm that EMS-11 is about the best that can be done given the present boundary conditions. Final testing of a uranium-containing version of EMS-11 is planned. Consideration of secondary criteria such as devitrification, phase separation, and electrical conductivity behavior will also be addressed.

SYNROC-C EVALUATION

Of the viable nonglass waste forms being considered as candidate second-generation high-level nuclear waste forms, Synroc-C has consistently exhibited very good performance. A series of comparative leach tests to evaluate Synroc-C relative to U-doped PNL 76-68 waste glass has been completed and the results are being compiled in a final report. Modified MCC-1 and MCC-2 tests were conducted using monolithic test specimens, and MCC-3 tests were conducted using specimens crushed to -40/+80 mesh (420 to 177 μm) to obtain a high surface area undisturbed by sawing. Tests were conducted at 90°C and 150°C in silicate water with a pH of 8.67 and brine with a pH of 4.43. The monolith tests were terminated at 28 days, but the MCC-3 powder tests were continued to 90 days. In addition to these tests, the temperature dependence on the forward leach rate was estimated between 90°C and 250°C in low surface area-to-volume tests conducted for 1 day. The PNL 76-68 glass contained 33 wt% PW-8a calcine and 4.16 wt% depleted UO_2 while Synroc-C contained 10 wt% PW-4b calcine and 0.50 wt% UO_2. This report summarizes some of the results obtained with leach tests using silicate water.

A preliminary evaluation of Synroc-C performance can be considered in terms of the release of Cs, Mo and U, which are common to both materials, and Ba, which is present only in Synroc-C. In monolith tests for up to 28 days, less than 1 ppm of Ba was released from Synroc-C and there was about a factor of three increase with temperature from 90 to 150°C at 28 days. The concentrations of Mo, Cs, and U in these monolith test leachates were normalized to the amount present in the waste form material. Normalized concentrations of Mo released from Synroc (2.0 g/m^2) were about an order of magnitude lower than from glass at 90°C. At 150°C, normalized Mo release was more than an order of magnitude higher in glass systems than in Synroc systems, which also showed very little temperature effect. Normalized Cs also showed very little temperature effect for Synroc with values of about 0.3 g/m^2 measured. Cs from glass systems was 20.0 g/m^2 at 90°C and 80.0 g/m^2 at 150°C. The normalized concentration of U from glass monoliths at 90°C was about 5.0 g/m^2 but only about 0.1 g/m^2 for Synroc. At 28 days, the data suggest that normalized U from Synroc in the 150°C tests may approach the values for glass, which may be

related to an initial supersaturation effect of U. Concentrations of U (not normalized) from high surface area-to-volume tests (MCC-3) yielded maximum values at about 28 days and then decreased as shown in Figure 12. These Synroc leachates were filtered through 0.5 μm and 1.8 nm filters; lack of change in the U concentration after filtration indicated that none of this U was in colloidal form. After 90 days leaching, filtration and re-analysis of glass leachates showed an order of magnitude decrease in U concentration, indicating that most of the U was colloidal.

Results from the MCC-3 powder leach tests indicated that Ba released from Synroc tends to form colloidal particles. Concentrations in filtrates through 0.5-μm paper were about 5 ppm and those through 1.8-nm paper were 1 ppm at 90°C. Cesium concentrations from powder tests reached steady-state values for both materials and were about 10 ppm in glass systems but 1 ppm in Synroc. This is probably a reflection of the different structural locations of Cs in the two waste forms. Molybdenum achieved a steady-state concentration of

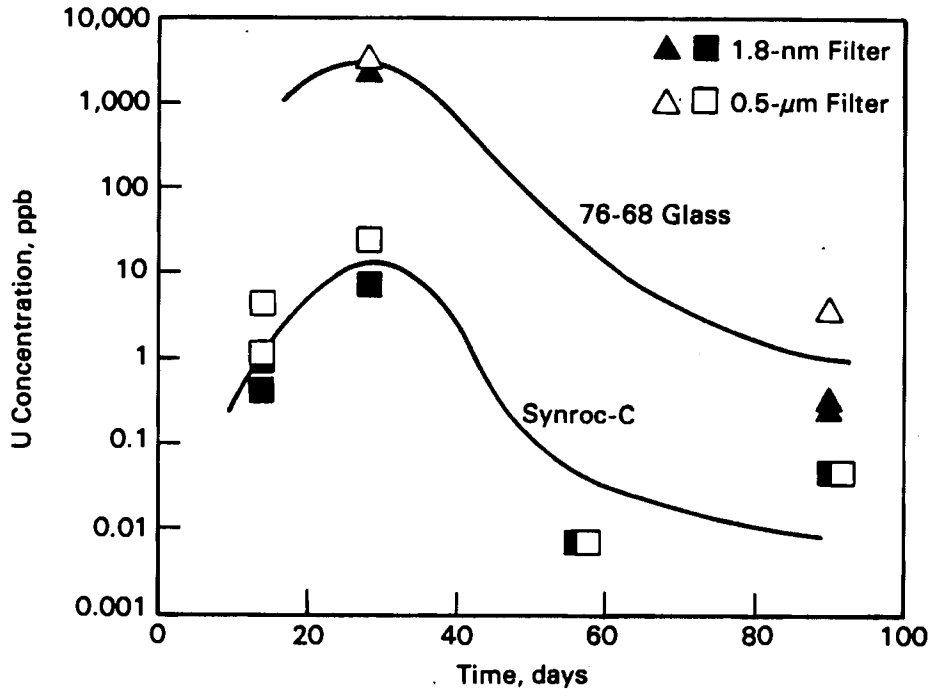

FIGURE 12. Uranium Concentrations in Silicate Water Leachates from Synroc-C and PNL 76-68 Glass Powder Tests at 90°C

10 ppm in Synroc powder tests at 90°C; at 90 days the Mo concentration was higher by about a factor of five in glass and showed no evidence of reaching steady state.

The temperature dependence for the forward release rate of Mo and Cs was estimated for both waste forms between 90 and 250°C by conducting 1-day dissolution tests at low surface area-to-volume ratios. In glass systems, initial release rates were about two to three orders of magnitude higher than in Synroc. Activation energies determined from Cs release rates from glass were the same as those determined from Mo release rates and had a value of about 8.7 kcal/mol. Activation energies determined from Cs release rates from Synroc were 3.2 kcal/mol while those determined from Mo release rates were 1.3 kcal/mol. This is an indication that Cs and Mo are associated with separate phases in Synroc.

CONCLUSIONS

The overview report of the West Valley vitrification system design provides the design bases and rationale for the equipment design. This perspective is useful for the West Valley project and for transfer of technology to other applications. Similar reports that provide the decision rationale for glass composition, feed composition, and nonradioactive melter operation should be considered.

Data collection will continue for the EMS, and chemical durability behavior will be modeled as a function of a (SA/V) x time related to flux composition. If successful, these models could be used to develop glasses that are tailored to anticipated repository conditions and requirements. At the present time, however, EMS-11 appears to have the potential of being a viable, significantly superior second-generation waste form. Preparation of a uranium and noble-metal-containing version of EMS-11 (EMS-11R) is planned for the next quarter. The EMS-11R glass will be evaluated for its viscosity, electrical conductivity, devitrification, phase separation, and chemical durability in various leachates.

Synroc-C appears to be a better waste form than a PNL 76-68-type borosilicate glass based on leach test performance but not necessarily on waste loading capacity. The concentration of some nuclides, such as uranium, that typically form low solubility reaction products may be controlled more by the type of reaction product than by release from the waste form.

REFERENCES

Blair, H. T., and M. E. Peterson. 1984. "A Pump for Metering High-Level Waste and Glass-Former Mixtures to an Electric Melter." In Proceedings International Topical Meeting on Fuel Processing and Waste Management, August 26-29, 1984, Jackson, Wyoming, p. 2-39.

Hilliard, R. K., et al. 1981. Submerged Gravel Scrubber Demonstration as a Passive Air Cleaner for Containment Venting and Purging with Sodium Aerosols. HEDL-TME 81-30, Hanford Engineering Development Laboratory, Richland, Washington.

Ludwig, E. E. 1980. Applied Process Design for Chemical and Petro-Chemical Plants. Vol. 1, 2nd ed. Crelf Publishing Co.

Siemens, D. H., et al. 1986. Design and Operating Features of the High-Level Waste Vitrification System for the West Valley Demonstration Project. PNL-5780, Pacific Northwest Laboratory, Richland, Washington.

APPENDIX

ACRONYMS AND ABBREVIATIONS

APPENDIX

ACRONYMS AND ABBREVIATIONS

Å - angstrom
ADS - air displacement slurry (pump)
Ag - silver
Al - aluminum
Am - americium
atm - atmosphere
B - boron
Ba - barium
Be - beryllium
C - carbon
°C - degree Celsius
Ca - calcium
cc - cubic centimeter
Cd - cadmium
Ce - cerium
Cl - chlorine
Ci - curie
cm - centimeter
Co - cobalt
cP - centipoise
Cr - chromium
CRW - cladding removal waste
Cs - cesium
Cu - copper
DF - decontamination factor
DOE - U.S. Department of Energy
DOE-DP - DOE-Defense Programs
DOE-NE - DOE-Nuclear Energy
DWPF - Defense Waste Processing Facility
Dy - dysprosium
ECM - experimental-scale ceramic melter
EDX - energy-dispersive x-ray
Eu - europium
EVS - ejector venturi scrubber
F - fluorine
Fe - iron
FRG - Federal Republic of Germany
ft - feet
FY - fiscal year
g - gram
gal- gallon
Gd - gadolinium
h - hour

H - hydrogen
HBCM - high-bay ceramic melter
HEME - high-efficiency mist eliminator
HEPA - high-efficiency particulate air (filter)
HIAC -
HLW - high-level waste
hp - horsepower
HWVP - Hanford Waste Vitrification Program
IAEA - International Atomic Energy Agency, Vienna, Austria
ICP - inductively coupled plasma
in. - inches
K - degree Kelvin
K - potassium
KEH - Kaiser Engineers Hanford Company, Richland, Washington
kg - kilogram
km - kilometer
kW - kilowatt
L - liter
La - lanthanum
lb - pound
LFCM - liquid-fed ceramic melter
Li - lithium
LLW - low-level waste
m - meter
M - molar
MCC - Materials Characterization Center, PNL
MEVS - Mobile Encapsulation and Volume Reduction System
mg - milligram
Mg - magnesium
min - minute
mL - milliliter
mm - millimeter
Mn - manganese
Mo - molybdenum
MTU - metric ton uranium
N - nitrogen
Na - sodium
Nb - niobium
NCAW - neutralized current acid waste
Nd - neodymium
Ni - nickel
Np - neptunium
NRC - U.S. Nuclear Regulatory Commission
NWTP - Nuclear Waste Treatment Program
O - oxygen
P - phosphorus
Pa - Pascal
Pb - lead
Pd - palladium
Pm - promethium
PNL - Pacific Northwest Laboratory, Richland, Washington

Pr - praseodymium
PSCM - pilot-scale ceramic melter
psig - pounds per square inch gauge
Pu - plutonium
Ra - radium
Rb - rubidium
RE - rare earth
Re - rhenium
Rh - rhodium
RLFCM - radioactive liquid-fed ceramic melter
rpm - revolutions per minute
Ru - ruthenium
s - second
S - sulfur
SA/V - surface area/volume ratio
Se - selenium
SEM - scanning electron microscope
Sn - tin
Si - silicon
Sm - samarium
Sr - strontium
SRL - Savannah River Laboratory, Aiken, South Carolina
T100P - temperature at which the glass has a 100 poise viscosity
Ta - tantalum
Tc - technetium
Te - tellurium
TDR - time domain reflectometer
Th - thorium
Ti - titanium
TRUW - transuranic waste
U - uranium
WC - water column
wt% - weight percent
WVDP - West Valley Demonstration Project
WVNS - West Valley Nuclear Services
Y - yttrium
yr - year
Zn - zinc
Zr - zirconium

DISTRIBUTION

No. of Copies

OFFSITE

30 DOE Technical Information Center

6 Geologic Repository Division
DOE Office of Civilian
Radioactive Waste Management
Forrestal Building
Washington, DC 20585
ATTN: C. R. Cooley, RW-4
J. R. Hilley
W. J. Purcell, RW-20
B. C. Rusche, RW-1
D. E. Shelor
R. Stein, RW-23

3 DOE Office of Defense Waste &
Byproducts Management
GTN
Washington, DC 20545
ATTN: R. K. Heusser
J. E. Lytle, DP-12
R. D. Walton, Jr., DP-123

6 DOE Office of Terminal Waste
Disposal & Remedial Action
GTN
Washington, DC 20545
ATTN: J. A. Coleman, NE-25
T. W. McIntosh, NE-25
H. E. Stelling, NE-25
W. R. Voigt, NE-20
H. F. Walter, NE-25

A. T. Clark
Division of Fuel Material Safety
Nuclear Regulatory Commission
Washington, DC 20555

V. Stello
Office of the Executive
Director for Operations
Mail Station 6209
Nuclear Regulatory Commission
Washington, DC 20555

No. of Copies

G. L. Sjoblom
Environmental Protection Agency
Office of Radiation Programs
401 M Street, S.W.
Washington, DC 20460

J. M. McGough
DOE Albuquerque Operations
Office
P.O. Box 5400
Albuquerque, NM 87185

P. G. Hagan
Joint Integration Office
Bldg. 3, 2nd Floor
2201 San Pedro N.E.
Albuquerque, NM 87110

E. Maestas
DOE West Valley Operations
Office
P.O. Box 191
West Valley, NY 14171

2 DOE Idaho Operations Office
550 Second Street
Idaho Falls, ID 83401
ATTN: M. J. Barainca
J. P. Hamric

F. T. Fong
DOE San Francisco Operations
1333 Broadway
Oakland, CA 94612

M. R. Jugan
DOE Oak Ridge Operations Office
P.O. Box E
Oak Ridge, TN 37830

W. J. Brumley
DOE Savannah River Operations
Office
P.O. Box A
Aiken, SC 29801

No. of Copies

M. J. Steindler
Argonne National Laboratory
9700 South Cass Avenue
Argonne, IL 60439

C. S. Abrams
Argonne National Laboratory
P.O. Box 2528
Idaho Falls, ID 83401

B. D. Shipp
Battelle Memorial Institute
Office of Crystalline Repository Development
9800 South Cass Avenue
Argonne, IL 60439

3 Battelle Memorial Institute
Project Management Division
505 King Avenue
Columbus, OH 43201
ATTN: W. A. Carbeiner
W. S. Madia
B. Rawles

F. Holzer
Lawrence Livermore National Laboratory
University of California
P.O. Box 808
Livermore, CA 94550

D. T. Oakley, MS 671
Los Alamos Scientific Laboratory
P.O. Box 1663
Los Alamos, NM 87544

4 Oak Ridge National Laboratory
P.O. Box Y
Oak Ridge, TN 37830
ATTN: J. O. Blomeke
W. D. Burch
R. T. Jubin
L. J. Mezga

No. of Copies

2 Sandia Laboratories
P.O. Box 5800
Albuquerque, NM 87185
ATTN: R. W. Lynch
Technical Library

J. R. Berreth
Westinghouse Idaho Nuclear Co., Inc.
P.O. Box 4000
Idaho Falls, ID 83401

6 E. I. du Pont de Nemours Company
Savannah River Laboratory
Aiken, SC 29801
ATTN: M. D. Boersma
J. G. Glasscock
E. J. Hennelly
J. R. Knight
M. J. Plodinec
C. T. Randall

E. A. Jennrich
EG&G Idaho
P.O. Box 1625
Idaho Falls, ID 83415

R. Williams
Electric Power Research Institute
3412 Hillview Avenue
P.O. Box 10412
Palo Alto, CA 94304

5 West Valley Nuclear Services Company
P.O. Box 191
West Valley, NY 14171
ATTN: C. C. Chapman
J. C. Cwynar
J. E. Krauss
S. J. Marchette
J. M. Pope

No. of
Copies

J. L. Larocca, Chairman
Energy Research & Development
Authority
Empire State Plaza
Albany, NY 12223

ONSITE

9 DOE Richland Operations Office

J. H. Anttonen
E. A. Bracken
G. J. Bracken
C. R. DeLannoy
R. D. Izatt
N. T. Karagianes
J. L. Rhoades
M. W. Shupe
J. D. White

10 Rockwell Hanford Operations

R. N. Gurley
J. M. Henderson
H. E. McGuire
R. D. Prosser
I. E. Reep
J. C. Scott
T. B. Venziano
D. D. Wodrich
R. D. Wojtasek
File Copy

UNC United Nuclear Industries

T. E. Dabrowski/W. J. Kyriazis

2 Westinghouse Hanford Company

R. E. Lerch
J. D. Watrous

63 Pacific Northwest Laboratory

C. R. Allen
W. W. Ballard, Jr.
S. O. Bates

No. of
Copies

H. T. Blair
W. F. Bonner
D. J. Bradley
R. A. Brouns
G. H. Bryan
H. C. Burkholder (10)
J. R. Carrell
D. B. Cearlock
R. D. Dierks
S. K. Edler
L. J. Ethridge
D. W. Faletti
R. K. Farnsworth
D. S. Goldman
R. W. Goles
H. A. Haerer
L. K. Holton
J. H. Jarrett
D. E. Knowlton
M. R. Kreiter
W. L. Kuhn
W. W. Laity
L. T. Lakey/K. M. Harmon
J. M. Latkovich
J. L. McElroy
G. L. McVay
J. E. Mendel/M. D. Merz
G. B. Mellinger
J. E. Minor
D. R. Montgomery
L. G. Morgan
T. R. Myers
J. M. Perez, Jr.
R. D. Peters
M. E. Peterson
A. M. Platt/R. E. Nightingale
J.T.A. Roberts
J. V. Robinson
W. A. Ross
K. J. Schneider
G. J. Sevigny
J. W. Shade
D. H. Siemens
J. L. Straalsund
J. H. Westsik, Jr.
Publishing Coordination (2)
Technical Information (5)